Simulating the evolution of Hardangerjøkulen ice cap in southern Norway since the mid-Holocene and its sensitivity to climate change

Henning Åkesson[1,2], Kerim H. Nisancioglu[1,3], Rianne H. Giesen[4], and Mathieu Morlighem[2]

[1]Department of Earth Science, University of Bergen and Bjerknes Centre for Climate Research, Allégaten 70, 5007 Bergen, Norway
[2]University of California, Irvine, Department of Earth System Science, 3218 Croul Hall, Irvine, CA 92697-3100, USA
[3]Centre for Earth Evolution and Dynamics, University of Oslo, Postbox 1028 Blindern, 0315 Oslo, Norway
[4]Institute for Marine and Atmospheric research, Utrecht University, P.O. Box 80005, 3508 TA Utrecht, The Netherlands

Correspondence to: Henning Åkesson (henning.akesson@uib.no)

Abstract. Understanding of long-term dynamics of glaciers and ice caps is vital to assess their recent and future changes, yet few long-term reconstructions using ice flow models exist. Here we present simulations of the maritime Hardangerjøkulen ice cap in Norway from the mid-Holocene through the Little Ice Age (LIA) to the present-day, using a numerical ice flow model combined with glacier and climate reconstructions.

In our simulation, under a linear climate forcing, we find that Hardangerjøkulen grows from ice-free conditions in the mid-Holocene to its maximum extent during the LIA in a non-linear, spatially asynchronous fashion. During its fastest stage of growth (2300–1300 BP), the ice cap triples its volume in less than 1000 years. The modelled ice cap extent and outlet glacier length changes from the LIA until today agree well with available observations.

Volume and area for Hardangerjøkulen and several of its outlet glaciers vary out-of-phase for several centuries during the Holocene. This volume-area disequilibrium varies in time and from one outlet glacier to the next, illustrating that linear relations between ice extent, volume and glacier proxy records, as generally used in paleo-climatic reconstructions, have only limited validity.

We also show that the present-day ice cap is highly sensitive to surface mass balance changes and that the effect of the ice cap hypsometry on the mass balance-altitude feedback is essential to this sensitivity. A mass balance shift by +0.5 m w.e. relative to the mass balance from the last decades almost doubles ice volume, while a decrease of 0.2 m w.e. or more induces a strong mass balance-altitude feedback and makes Hardangerjøkulen disappear entirely. Furthermore, once disappeared, an additional +0.1 m w.e. relative to the present mass balance is needed to regrow the ice cap to its present-day extent. We expect that other ice caps with comparable geometry in for example Norway, Iceland, Patagonia and peripheral Greenland may behave similarly, making them particularly vulnerable to climate change.

1 Introduction

The 211,000 glaciers and ice caps (GICs) (Pfeffer et al., 2014; Arendt et al., 2015) in the world are relatively small compared to the Greenland and Antarctic ice sheets, but they constitute about half of the current cryospheric contribution to sea level rise

(Shepherd et al., 2012; Vaughan et al., 2013), a distribution projected to remain similar throughout the 21st century (Church et al., 2013; Huss and Hock, 2015). Since areas of GICs are more readily available than their volume, scaling methods are commonly employed to estimate total ice volumes and their sea level equivalents (e.g. Bahr et al., 1997; Grinsted, 2013; Bahr et al., 2015). Many of these GICs are ice caps, though little is known about their response to long-term climate change, how a

5 particular ice cap geometry contributes to this sensitivity or how scaling methods perform for ice caps.

Reconstructions of past climate and glacier variations contribute to our understanding of long-term glacier behavior. However, these studies often build on simple glaciological assumptions relating proxies, ice extent, ice volume and climate (e.g. Hallet et al., 1996). As glaciers are non-linear systems with feedbacks, such relations are difficult to constrain without a numerical model. Yet long-term reconstructions using ice flow models are rare. Most existing quantitative modelling studies of

10 GICs are restricted to timescales of decades (e.g. Leysinger-Vieli and Gudmundsson, 2004; Raper and Braithwaite, 2009) or centuries (Jouvet et al., 2009; Giesen and Oerlemans, 2010; Adalgeirsdóttir et al., 2011; Zekollari et al., 2014; Zekollari and Huybrechts, 2015; Ziemen et al., 2016). Only a very limited number of studies exist for the longer timescales (e.g. Flowers et al., 2008; Laumann and Nesje, 2014). Studies focusing on glacier evolution since the Little Ice Age (LIA) (e.g. Giesen and Oerlemans, 2010; Adalgeirsdóttir et al., 2011; Zekollari et al., 2014) normally perturb a present-day glacier or ice cap with a

15 climate anomaly relative to the modern and do not explicitly consider the ice cap history preceding the LIA.

In this study, we use a numerical ice flow model to provide a quantitative, long-term, dynamical perspective on the history and current state of the Hardangerjøkulen ice cap in southern Norway. These results are also relevant for our understanding of the history and future stability of similar ice masses in e.g. Norway (Nesje et al., 2008a), Iceland (Adalgeirsdóttir et al., 2006), Patagonia (Rignot et al., 2003), Alaska (Berthier et al., 2010) and peripheral Greenland (Jacob et al., 2012). We present

20 a plausible ice cap history over several thousand years before the LIA (Sect. 4.1), and use this as a starting point for simulations from LIA to present-day (Sect. 4.2). To evaluate the sensitivity of the ice cap to the choice of dynamical model parameters, we perform an ensemble of simulations with different dynamical model parameters (Sect. 4.2.1). Furthermore, we quantify the sensitivity of Hardangerjøkulen to climatic change (Sect. 4.3).

We find that Hardangerjøkulen is exceptionally sensitive to surface mass balance changes, and that the surface mass balance-

25 altitude feedback and ice cap hypsometry is crucial to this sensitivity. To constrain the assumptions made in glacier reconstructions and volume-area scaling applications, we assess the degree of linearity between ice cap volume and area (Sect. 4.4). We show that commonly used scaling relations overestimate ice volume, and suggest that glacier and climate reconstructions could benefit from quantifying the impact on proxy records of bed topography, glacier hypsometry and the surface mass balance-altitude feedback (Sect. 5.5).

2 Hardangerjøkulen ice cap

2.1 Present-day geometry

2.1.1 Surface topography

Hardangerjøkulen (60°55'N, 7°25'E) has a present-day (year 2012) area of 73 km^2 (Andreassen et al., 2012) and is located at the western flank of the Hardangervidda mountain plateau. The ice cap is rather flat in the interior with steeper glaciers draining the plateau (Fig. 1). The largest outlet glaciers are Rembesdalskåka (facing W-SW; 17.4 km^2), Midtdalsbreen (NE; 6.8 km^2), Blåisen (NE; 6.6 km^2) and Vestre Leirbotnskåka (S-SE; 8 km^2). Surface elevation ranges from 1020 to 1865 m a.s.l. (Andreassen et al., 2015), with 80 % of the ice cap area, and 70 % of Rembesdalskåka, situated above the mean equilibrium-line altitude (ELA) at 1640 m a.s.l. (1963-2007 average; Giesen, 2009). Rembesdalskåka drains towards the dammed lake Rembesdalsvatnet, located ~1 km from the present-day glacier terminus (Kjøllmoen et al., 2011). Midtdalsbreen is a gently sloping outlet glacier ranging from 1380 to 1865 m a.s.l.

2.1.2 Ice thickness and bed topography

A number of surveys have mapped the ice thickness at Hardangerjøkulen (e.g. Sellevold and Kloster, 1964; Elvehøy et al., 1997; Østen, 1998, K. Melvold, unpubl. data), with the highest measurement density for Midtdalsbreen (Fig. 2.12a in Giesen, 2009; Willis et al., 2012). In areas with dense measurements, ice thickness was interpolated using methods detailed in Melvold and Schuler (2008). In sparsely measured areas, ice thickness H was estimated directly from the surface slope α, assuming perfect plasticity (Paterson, 1994, p. 240). Based on detailed ice thickness measurements and information on the surface slope on Midtdalsbreen, a yield stress of 150-180 kPa was used, in agreement with other mountain glaciers (Cuffey and Paterson, 2010, p.297; Zekollari et al., 2013). Over the flat areas near ice divides and ice ridges, as well as near ice margins, manual extrapolation was required to obtain a smooth ice surface (K. Melvold, pers. comm.). A map of bed topography (Fig. 1) was produced by combining the final ice thickness map with a surface DEM (year 1995) from the Norwegian Mapping Authority, derived from aerial photographs.

2.2 Past geometry

2.2.1 Holocene changes

Reconstructions show that glaciers in southern Norway did not survive the mid-Holocene thermal maximum (e.g. Bakke et al., 2005; Nesje, 2009). Based on lake sediments and terrestrial deposits, Hardangerjøkulen is estimated to have been absent from circa (c.) 7500 to 4800 BP (Dahl and Nesje, 1994), although a short-lived glacier advance is documented for the southern side of the ice cap at c. 7000 BP (Nesje et al., 1994). Some high-frequency glacier fluctuations of local northern glaciers occurred during the period 4800-3800 BP, after which Hardangerjøkulen has been present continuously (Dahl and Nesje, 1994). There are few quantitative constraints on ice cap extent for the period from ice cap inception 4000 BP until the LIA. However,

interpretations of lake sediments and geomorphological evidence suggest a gradual growth of Hardangerjøkulen during this period (Dahl and Nesje, 1994, 1996).

2.2.2 Outlet glacier changes since the Little Ice Age

Length changes extracted from maps and satellite imagery, moraine positions and direct front measurements are combined to derive length records for two major outlet glaciers for the period 1750-2008. For Rembesdalskåka, we use the same flowline as the Norwegian Water and Energy Directorate (NVE) use for their mass balance measurements (H. Elvehøy, pers. comm.). The NVE flowline for Midtdalsbreen was slightly modified to better correspond with the maximum ice velocities. Since changes are only made upglacier of the present-day margin, they do not interfere with the area where data of frontal changes exist.

The LIA maximum for Midtdalsbreen is dated to 1750 AD with lichenometry (Andersen and Sollid, 1971). For Rembesdalskåka, the outermost terminal moraine has not been dated, but is assumed to originate from the LIA maximum.

Frontal observations for Rembesdalskåka began in 1917. These have been performed for 22 of the years during the period 1917-1995, and are since 1995 done annually. For Midtdalsbreen, an annual length change record exists from 1982 onwards (Kjøllmoen et al., 2011). At present, Rembesdalskåka has retreated almost 2 km from its LIA maximum extent and Midtdalsbreen ∼1 km.

The two outlet glaciers considered advanced in response to snowy winters around 1990. The terminus change from 1988 to 2000 for Rembesdalskåka was +147 m and for Midtdalsbreen +46 m. By 2013, Rembesdalskåka and Midtdalsbreen had retreated 332 m and 164 m respectively, from their positions in 2000 (Andreassen et al., 2005; Kjøllmoen et al., 2011; Cryoclim.net, 2014).

2.3 Climate

2.3.1 Holocene and Little Ice Age climate

Reconstructions for southern Norway based on pollen and chironomids suggest that summer temperatures were up to 2°C higher than present in the period between 8000–4000 BP, when solar insolation was higher (Nesje and Dahl, 1991; Bjune et al., 2005; Velle et al., 2005a). At 4000 BP, proxy studies suggest a drop in summer temperatures to 0.5 °C lower than present combined with a drier climate (Dahl and Nesje, 1996; Bjune et al., 2005; Velle et al., 2005b; Seppä et al., 2005).

Dahl and Nesje (1996) reconstructed Holocene summer temperatures for southern Norway based on former pine-tree limits. Using a well-established empirical relationship between summer temperature and winter precipitation at the ELA of Norwegian glaciers (Liestøl in Sissons, 1979; Sutherland, 1984), they estimated winter precipitation for the Hardangerjøkulen area from lake sediment-derived ELAs. These reconstructions suggest a close to linear cooling and wetting trend from 4000 BP until the LIA, including a possible warm event lasting for several centuries around 2000 BP (Velle et al., 2005a).

The LIA climate in southern Norway is likely to have experienced more precipitation (Nesje and Dahl, 2003; Nesje et al., 2008b; Rasmussen et al., 2010) and was c. 0.5-1.0 °C colder than present (Kalela-Brundin, 1999; Nordli et al., 2003), although some reconstructions indicate milder summers during the first quarter of the 18th century (Kalela-Brundin, 1999).

2.3.2 Present climate

Southern Norway is located in the Northern Hemisphere westerly wind belt and is heavily influenced by moist, warm air picked up by the frequent storms coming off the Atlantic Ocean (Uvo, 2003). When these winds reach the mountainous west coast, orographic lifting occurs and precipitation falls as rain or snow, depending on elevation. Conversely, eastern Norway is located in the rain shadow of the coastal mountains and the high mountain plateau Hardangervidda.

This strong west-east precipitation gradient is illustrated by the mean annual precipitation for 1961-1990 over southern Norway. Precipitation in Bergen, 65 km west of Hardangerjøkulen, reaches 2250 mm a^{-1} (data from eklima.no, Norwegian Meteorological Institute). In contrast, Oslo in eastern Norway receives 763 mm precipitation per year. Liset, 17 km southeast of the summit of Hardangerjøkulen receives 1110 mm a^{-1}, while Finse, 8 km northeast of the summit, experiences 1030 mm a^{-1}. Finse has a mean annual temperature of -2.1°C, while temperature is not measured at Liset.

2.4 Surface mass balance

Glaciological mass balance measurements started on Rembesdalskåka in 1963. The mean net balance for the period 1963–2010 was slightly positive (+0.08 m water equivalent (w.e.)), divided into a winter balance of +2.10 m w.e. and a summer balance of -2.03 m w.e. (Kjøllmoen et al., 2011).

For Midtdalsbreen, mass balance was only measured in 2000 and 2001 (Krantz, 2002). This two-year time series is too short for a robust surface mass balance comparison between the two outlet glaciers.

Specific mass balance profiles for the entire elevation range of Rembesdalskåka exist for 35 of the 45 mass balance years (October 1 - September 30) in the period 1963–2007. The interannual variability around the mean winter profile is similar at all elevations, while the range in summer balances increases from high to low elevations (Fig. 2.7a in Giesen, 2009). The decrease in mass balance at the highest elevations is a persistent feature of the winter mass balance, and is strongest in years with large accumulation (Fig. 5.3 in Giesen, 2009). Its origin is however uncertain and long-term snow depth measurements on several outlet glaciers are needed to identify the underlying process.

The net balance profile has a similar shape for most years, and the relation between net mass balance and altitude is approximately linear from the terminus up to 1675 m a.s.l. (Fig. 2), with a mass balance gradient of 0.0097 m w.e. per m altitude. The net mass balance is zero at 1640 m a.s.l., marking the ELA. Above the ELA, the mass balance gradient decreases with altitude, and becomes negative at the highest elevations (Fig. 2).

2.5 Ice dynamics

2.5.1 Basal conditions

Although bed conditions are not well-known, based on the sparse sediment cover in the surrounding areas (Andersen and Sollid, 1971), we assume Hardangerjøkulen to be hard-bedded, i.e. without any deformable subglacial sediments present.

Given its climatic setting and based on the radar investigations described in Sect. 2.1.2, Hardangerjøkulen can be characterized as a temperate ice cap. To the contrary, temperature measurements suggest that Midtdalsbreen has local cold-based areas at its terminus (Hagen, 1978; Konnestad, 1996; Reinardy et al., 2013). However, we expect that this has a minor effect on the large scale ice flow of Midtdalsbreen and Hardangerjøkulen.

2.5.2 Surface velocities

Over the lower ablation zone of Midtdalsbreen, surface speeds of 4–40 m a^{-1} were measured during summer 2000 (Vaksdal, 2001). In addition, ice velocities were derived from Global Positioning System (GPS) units recording at nine locations on Hardangerjøkulen during the period May 2005–September 2007 (Giesen, 2009). One GPS was mounted on the automatic weather station (AWS) on Midtdalsbreen, the other eight were situated on stakes at the ELA of the main outlet glaciers (Fig. 1). These data show highest velocities for the largest outlet glacier Rembesdalskåka (46 m a^{-1}). Velocities at Midtdalsbreen, measured May 2005 to March 2006, were 33 m a^{-1} at the ELA and ∼20–22 m a^{-1} at the AWS, which is within the range of ablation zone summer velocities suggested by Vaksdal (2001).

Since velocities have only been measured for single years or shorter, these observations provide guidance rather than serving as calibration or validation data for our model. To the authors' knowledge, there are no high resolution velocity data derived from remote sensing covering the area of interest.

3 Model description and setup

3.1 Ice flow model

We use the two-dimensional, vertically integrated Shallow Ice Approximation (SIA) within the finite-element Ice Sheet System Model (ISSM; Larour et al., 2012). Only the capabilities of ISSM relevant for this paper are covered here, for a complete description, including a more comprehensive section on model numerics and architecture, we refer to Larour et al. (2012) and http://issm.jpl.nasa.gov.

The SIA is based on a scaling analysis of the Stokes stress balance (Hutter, 1983; Morland, 1984). This scaling argument assumes that the typical glacier length L, is much larger than the typical ice thickness H. For this purpose, the aspect-ratio ϵ is defined as

$$\epsilon = \frac{[H]}{[L]}, \tag{1}$$

where ϵ describes the 'shallowness' of an ice mass. An aspect-ratio much smaller than unity is required for the SIA to be valid. Generally, the smaller the ϵ, the more accurate the SIA is (Le Meur et al., 2004; Greve and Blatter, 2009; Winkelmann et al., 2011). Based on outlet glacier length records from the LIA until today, the characteristic horizontal scale for Hardangerjøkulen is 4 to 10 km. Due to the highly variable bed topography, a typical vertical scale of ∼200 m is estimated qualitatively using ice thickness around the ELA. These scales give an ϵ between 0.02 and 0.05, which is acceptable for using the SIA (Le Meur and Vincent, 2003).

The SIA has proven accurate in representing glacier length and volume fluctuations on the decadal and longer time scales we are focusing on (Leysinger-Vieli and Gudmundsson, 2004). While higher order models may be needed in dynamic regions, even for paleosimulations (Kirchner et al., 2016), Hardangerjøkulen has relatively gentle surface slopes and lacks areas of very fast flow, making the SIA a viable choice.

5 Because of its simplicity, SIA is also computationally efficient (Rutt et al., 2009), enabling ensemble simulations over longer time scales.

3.1.1 Ice deformation and sliding

The constitutive relationship relating stress to ice deformation (strain rate) is Glen's flow law (Glen, 1955), which for the special case of vertical shear stress τ_{xz} only (SIA) states

$$\dot{\epsilon} = A\tau_{xz}^n, \tag{2}$$

where $\dot{\epsilon}$ is the strain rate tensor, A is the flow factor accounting for ice rheology and $n = 3$ is Glen's flow law exponent. We use a spatially constant flow factor A, assuming homogeneous ice temperature T_{ice} and material properties across the ice cap.

In contrast to many other studies, where a tuned 'best-fit' parameter combination is selected and used in all simulations, we perform ensemble runs for a parameter space of different flow factors and sliding parameters (described below), for both the 15 calibration procedure and subsequent model runs.

SIA is strictly only valid for a no-slip bed (Gudmundsson, 2003; Hindmarsh, 2004). However, Hardangerjøkulen is a temperate ice cap, and summer speed-ups have been observed at Midtdalsbreen (Willis, 1995; Willis et al., 2012), indicating basal motion. We introduce sliding using a linear Weertman sliding formulation (Weertman, 1964), which for the SIA means basal velocities u_b are proportional to the basal shear stress τ_b:

$$u_b = \beta\tau_b^m, \tag{3}$$

where β is a (tuning) basal sliding parameter. β can be set spatially and temporally constant, or be a function of temperature, basal water depth, basal water pressure, bed roughness or other factors, and m is the sliding law exponent, which equals one for the linear sliding law we apply.

In this study, the basal sliding parameter β is assumed spatially and temporally constant. We consider it speculative to apply 25 *ad-hoc* variations in basal sliding without proper validation. ISSM has capabilities to perform inversions for basal friction based on data assimilation techniques (e.g. MacAyeal, 1993; Morlighem et al., 2010), but this requires more extensive velocity data coverage than what is available for Hardangerjøkulen at present. More fundamentally, inverted friction fields may become inaccurate on the long time scales considered in this study.

3.1.2 Mass transport

30 For the vertically-integrated ice flow model used in this study, the two-dimensional continuity equation states

$$\frac{\partial H}{\partial t} = -\nabla \cdot (\bar{u}H) + \dot{M}, \tag{4}$$

where $\bar{u}$ is the vertically averaged ice velocity (m a^{-1}) and $\dot{M}$ the surface mass balance rate (m ice equivalent a^{-1}). The basal melt rate is assumed negligible, and calving is not included in the model. Rembesdalskåka likely terminated in lake Rembesdalsvatnet during the LIA and the northwestern ice cap presently terminates in water, however we expect this to have minor effect on ice dynamics.

3.1.3   Mesh and time stepping

Following methods outlined in Hecht (2006) and Morlighem et al. (2011), an anisotropic mesh with resolution 200-500 m was constructed using local mesh refinement based on modelled velocities for a steady-state ice cap close to observed LIA extent. This ice cap was reached using our 'best-fit' deformation and sliding parameters (Sect. 3.2.1) on a uniform mesh, and a mass balance perturbation forcing the ice cap to advance to terminus positions close to the LIA extent. The anisotropic mesh adds accuracy around the LIA margins. When the glacier is smaller or larger, the accuracy is reduced (400-500 m).

The stress balance of SIA is local. Using a very high resolution for SIA hence increases the risk of unphysical stress gradients and velocities due to local variations in bed topography. We avoid this by smoothing the surface and bedrock DEM's to 200 m. This mesh resolution also enables us to carry out Holocene runs and our ensemble study at lower computational cost. Tests on mesh convergence using uniform 150 m and 200 m meshes indicate that total volume varies by less than 5 % compared to our anisotropic 200-500 m mesh.

We use a finite difference scheme in time, where a time step of 0.02 years was found low enough to avoid numerical instabilities.

3.2   Experimental setup and calibration

3.2.1   Ensemble calibration of ice deformation and sliding parameters

To calibrate model parameters governing ice deformation and basal sliding, we use the 1995 surface DEM as the initial condition. We run the model with constant climate forcing, using our reference mass balance function ($\Delta B(t) = 0$ in Eq. 6 below), until a steady-state is reached.

Since we run the model with a mass balance function averaged over several decades, it is important that there was no large climate-geometry imbalance for this period. Indeed, the ice cap was in close to steady-state between the early 1960s and 1995, since surface elevation change from 1961 to 1995 was $\pm$ 10 m (Andreassen and Elvehøy, 2001).

In reality, an ice cap is never in exact steady-state, but it is still a useful concept to understand model sensitivity (Adalgeirsdóttir et al., 2011). To investigate model sensitivity to deformation and sliding parameters, and to find a 'best-fit' combination for our historic runs, we run an ensemble of 24 possible parameter combinations, well enclosed by values used in the literature. The flow factor A depends on ice temperature, as well on ice fabric, impurities and possibly other factors. Without an *a priori* assumption of ice temperature, we investigate values from $A = 0.95 \times 10^{-24}$ to 2.4×10^{-24} s^{-1} Pa^{-3}, roughly corresponding to $T_{ice} = 0$ to -5 °C (Cuffey and Paterson, 2010, p.73). For the sliding parameter, we perform runs using $\beta = 4 \times 10^{-12}$ to 1 $\times 10^{-13}$ m s^{-1}Pa^{-1}.

The 'best-fit' combination is obtained by minimizing the Root Mean Square Error (RMSE) between the modelled (H_{mod}) and observed (H_{obs}) ice thickness:

$$RMSE = \sqrt{\frac{\sum\limits_{i=1}^{k}(H_{mod} - H_{obs})^2,}{k}} \tag{5}$$

where k is the number of vertices for which the RMSE is calculated.

5   Since the outlet glaciers Midtdalsbreen and Rembesdalskåka are of primary interest, we use the combined RMSE along their flowlines as the most important metric (Fig. 3). As an additional check, we also calculate the RMSE for ice thickness over the entire ice cap (not shown here). We consider our 'best-fit' parameter combination to be $A = 2.0315 \times 10^{-24}$ s^{-1} Pa^{-3} and $\beta = 2 \times 10^{-12}$ m s^{-1}Pa^{-1} (Fig. 3).

3.2.2   Mass balance parametrization

10   A vertical reference mass balance function B_{ref} is derived from observed specific mass balance gradients, which exist for 35 of the 45 years spanning 1963–2007. The averaged net mass balance profile can be approximated by a combination of a linear function for elevations up to 1675 m a.s.l. and a third-order polynomial at higher elevations (Fig. 2). The resulting mass balance function gives an annual mass balance for Rembesdalskåka of -0.175 m w.e. We therefore shifted this profile by +0.175 m w.e. to obtain B_{ref}.

15   Mass balance $B(z,t)$ for any point in time is calculated by shifting B_{ref} by a mass balance anomaly $\Delta B(t)$ at all elevations (Oerlemans, 1997a):

$$B(z,t) = B_{ref}(z) + \Delta B(t). \tag{6}$$

A mass balance-altitude feedback is included in the model by recalculating the mass balance $B(z,t)$ at a specific point for each time step according to the updated surface elevation. The elevation of the maximum net mass balance is not adapted to 20   changes in the ice cap summit elevation, as the effect on modelled ice volume is minor (Giesen, 2009).

3.2.3   Holocene mass balance

Reconstructions (Sect. 2.2.2) suggest that Hardangerjøkulen has been continuously present since c. 3800 BP, with smaller local glacier activity during the millennium before. We therefore choose 4000 BP, with no ice cap present, as the starting point for our simulations.

25   Temperature proxies indicate a positive mass balance anomaly at 4000 BP, while precipitation reconstructions point to more negative mass balances (Sect. 2.2.2). Combined, these suggest mass balance conditions similar to present-day. Accordingly, we start from $\Delta B(t) = 0$ and thereafter linearly increase mass balance to 0.4 m w.e. over the period 4000 BP to 400 BP (1600 AD). The final value of 0.4 m w.e. is chosen to produce an ice cap sized between the present-day and LIA extent. For this simulation, we use our 'best-fit' deformation and sliding parameters obtained from the calibration ensemble.

It is possible to refine or alternate this simple forcing in several ways. However, applying such changes based on poorly constrained past climatic and mass balance conditions adds additional uncertainty. Our deliberately simple, linear forcing also allows us to isolate any non-linear, asynchronous behaviour in a clear manner.

3.2.4 Historic mass balance

5   Using our Holocene run ending at 1600 AD as initial conditions, we aim to reproduce the history of Hardangerjøkulen from the LIA until present-day, as well as to assess model sensitivity to the choice of deformation and sliding parameters. For these purposes, we run the same parameter ensemble as used in the calibration process.

Since the mass balance record from Rembesdalskåka starts in 1963, mass balance has to be reconstructed for the period prior to this. A plausible mass balance history is found from 1600 AD, through the LIA maximum in 1750 up to 1963, using
10   a dynamic calibration (Oerlemans, 1997a, 2001). This approach is based on matching the model against the moraine evidence and length records of the outlet glaciers Midtdalsbreen and Rembesdalskåka, while adjusting $\Delta B(t)$ accordingly. We use a slightly modified mass balance history as obtained for Hardangerjøkulen by Giesen (2009), using minimal tuning, since a key aim is to investigate parameter sensitivity, and mass balance is arbitrary before 1963.

3.2.5 Mass balance sensitivity and hysteresis

15   To investigate the sensitivity of present-day Hardangerjøkulen to changes in mass balance, steady-state experiments are performed with present-day ice cap topography as the starting point. These experiments are performed starting from the steady-state ice cap obtained with the 'best-fit' parameters and no mass balance anomaly. From this state, we perturb the mass balance by anomalies between -0.5 and +0.5 m w.e., and run the model to a new equilibrium.

To investigate the role of the mass balance-altitude feedback in the ice cap response, we perform additional experiments
20   excluding this feedback by keeping the spatial mass balance field fixed in time to the present-day surface topography.

Finally, we investigate dependence on initial conditions (hysteresis), by running experiments using ice-free initial conditions, with the mass balance-altitude feedback included.

4   Results

4.1   Mid- to late Holocene evolution of Hardangerjøkulen

25   Using a linear mass balance increase from 0 m w.e. at 4000 BP to 0.4 m w.e. at 1600 AD (Fig. 4a), we find an ice volume evolution for Hardangerjøkulen during the mid- to late Holocene that is far from linear and different between outlet glaciers (Fig. 4c). Starting from ice-free conditions, ice cap volume increases in a step-wise manner, with Hardangerjøkulen tripling its volume over a period of 1000 years (c. 2300–1300 BP), before stabilizing at the end of the period.

Simulated snapshot thickness maps reveal patterns of ice cap growth (Fig. 5). Initially, ice grows on high bedrock ridges
30   above the ELA (Fig. 5a, also see Fig. 1). During the period of linearly increasing ice volume (4000–3800 BP), Rembesdalskåka

and Midtdalsbreen advance at similar rates. At this stage, Rembesdalskåka occupies an area with a gently sloping and partly overdeepened bed (Fig. 6).

After passing the lower edge of this overdeepening, Rembesdalskåka advances ∼3.5 km in 400 years (2300–1900 BP), corresponding to a length increase of 60 % (Fig. 6). In contrast, Midtdalsbreen is already at an advanced position in 2300 BP, and changes only modestly during this period.

Ice volume grows rapidly from 2300–1900 BP, however the advance and thickening of Rembesdalskåka alone can not explain this ice volume increase. Rather, the bulk of Hardangerjøkulen's volume increase during this period is due to ice cap growth in the east and southeast, where deep bedrock basins are filled with ice up to 400 m thick (Fig. 5d, see also Fig. 1).

We tested alternative mass balance forcings (faster rate of linear increase, and constant mass balance equal to the final value), and found the spatial pattern of ice cap growth to be robust.

At the end of the spinup period (c. 1300–400 BP), outlet glaciers stabilize their frontal positions, and ice volume increase flattens out.

4.2 Hardangerjøkulen since the Little Ice Age

4.2.1 Parameter ensemble

From 1600 AD, we continue the Holocene run using our ensemble of sliding and deformation parameter combinations, for one specific mass balance history. The ensemble modelled ice volumes at the LIA maximum (1750 AD) range from c. 12.7 to 17.4 km^3, and vary between 6.9 and 13.4 km^3 for the present-day (2008 AD; Fig. 4d). Parameter combinations including rate factors $A(T = -1\,°C)$ all give results $\pm$ 10 % from the observed ice volumes in 1961 and 1995. Using enhanced sliding and stiffer ice, or vice versa, it is possible to get close to the observed ice volume also for other rate factors. However, only using ice volume for validation is not sufficient. A simulated ice volume close to observations does not imply accurate ice extent and surface topography. The ∼100 m spread in estimated surface elevation for the ice cap interior in 1995 (Fig. 7), illustrates the impact of parameter uncertainty on the dynamics and hence ice cap hypsometry.

4.2.2 Simulation using 'best-fit' parameters

The LIA maximum ice volume using the 'best-fit' parameter combination is modelled to 14.8 km^3 (Fig. 4d). It is not possible to obtain correspondence to observed lengths for both outlet glaciers simultaneously, not even by altering the dynamical parameters (Fig. 7). The mass balance history giving optimal results for Midtdalsbreen was chosen since its LIA maximum extent has been dated to 1750 AD, while no dates exist for Rembesdalskåka. In addition, bed topography is more accurate for Midtdalsbreen. Using this setup, the LIA maximum length agrees reasonably well with moraine evidence, whereas Rembesdalskåka is too short (Fig. 8). Consistent with the results for Midtdalsbreen and Rembesdalskåka, the lengths of the southwestern outlet glaciers at the LIA maximum are underestimated in the model (Fig. 9a), while the extent of the northeastern outlet glaciers agrees well with moraine evidence.

During the early 1900s, outlet glacier lengths are too short (Fig. 8 and 9b), but the difference for Midtdalsbreen is only slightly larger than the model resolution (200 m). The ice cap margin after 1960 is reproduced with a high degree of detail (Fig. 9cd). Most, but not all discrepancies are close to the model resolution. One exception is the too small northwestern ice cap. However, ice thickness in the missing area is small (< 50 m), so this mismatch contributes little in terms of total ice volume.

5   The closest match with observed ice volume in 1961 and 1995 (Fig. 4d) within our ensemble is by the 'best-fit' parameter combination obtained from calibration (Fig. 3). Modeled and observed ice volume for these years differ by 0.10 and 0.22 km^3, respectively, or 1.1 and 2.3 % of total observed ice volume, respectively. Modelled thickness in 1995 is generally in good agreement with the data, though the ice cap interior is somewhat too thin and the thickness along the eastern margin is overestimated (Fig. 9e).

10   The simulated continuous ice volume history of Hardangerjøkulen, from 4000 BP through the LIA until today, including our ensemble from 1600 AD onwards, is shown in its entirety in Fig. 4cd. The simulations show that Hardangerjøkulen has lost one-third of its volume between 1750 and present-day.

4.3 Mass balance sensitivity and hysteresis

We find that Hardangerjøkulen at present is exceptionally sensitive to mass balance changes (Figs. 10 and 11a). In particular,
15   the ice cap is bound to disappear almost entirely for mass balance anomalies of -0.2 m w.e. or lower. Our parameter ensemble suggests a disappearance for anomalies between -0.5 to -0.1 m w.e., though this range is likely smaller as explained in Sect. 4.2.1. Our simulations show a close to linear relationship between positive mass balance perturbations and ice volume response (Fig. 10), while the ice cap melts away partly or completely for the negative anomalies.

Further experiments show that the mass balance-altitude feedback is vital in explaining Hardangerjøkulen's high sensitivity
20   to climate change. Without the feedback, the ice cap responds close to linearly to mass balance perturbations and thus is far less sensitive to climate change (Fig. 11b). For example, half of present-day ice volume (4.9 km^3) is still present for a mass balance anomaly of -0.5 m w.e., while with +0.5 m w.e., ice volume increases by $\sim$35 %. In stark contrast, when including the feedback, the ice cap disappears completely for the corresponding negative anomaly, and ice volume almost doubles (+92 %) for the positive anomaly (Fig. 11a).

25   Starting from ice-free conditions and including the mass balance-altitude feedback, we find that the Hardangerjøkulen's climatic response depends on the ice cap's initial state. For mass balance anomalies close to our reference mass balance for 1963–2007, between -0.2 and +0.1 m w.e., large differences occur between ice volumes reached from present-day and ice-free conditions (Fig. 10). When starting from a situation without ice, present-day mass balance conditions produce an ice cap that has only 20% of the volume of today's ice cap. In addition to Hardangerjøkulen being bound to disappear almost completely
30   for a slight decrease in the mass balance, this result implies that a positive mass balance anomaly is needed to regrow the ice cap to its present-day extent, once it has disappeared.

4.4 Volume-area phasing and scaling

Our Holocene simulations show that the ice volume evolution for three of the outlet glaciers (Rembesdalskåka, Midtdalsbreen, Blåisen) is asynchronous (Fig. 12). Midtdalsbreen's ice volume increases linearly over time, while Rembesdalskåka and Blåisen have distinct jumps in ice volume, related to their bed topography. The importance of bedrock troughs and overdeepenings is further illustrated by Hardangerjøkulen's non-linear volume increase c. 2300–1300 BP, a period when volume increases faster than area (Fig. 12). During this period, ice is thickening rather than expanding horizontally, which can largely be explained by ice growth in subglacial valleys in the eastern and southeastern parts of the ice cap (Fig. 1). These bed depressions fill up quickly because ice flow converges into them from surrounding high bedrock ridges, and the mass balance-altitude feedback amplifies the ice thickening.

We compare our steady-state mass balance perturbation experiments (Sect. 4.3) with volume-area scaling relations for steady-state ice caps from the literature (Fig. 13a), of the form $V = cA^\gamma$ (Bahr et al., 1997). For a consistent comparison, we group our perturbation experiments into those which produce a fully developed ice cap, and those where ice is mainly present on high ridges, and thus cannot be classified as a glacier or ice cap. We find that ice cap scaling relations from the literature overestimate the ice volume of the full-grown ice cap. Both the exponent and the scaling factor found for Hardangerjøkulen (γ = 1.3738 and $c = 0.0227$) are closer to literature values for valley glaciers (e.g Bahr et al., 2015).

During the first half of the Holocene simulation, a full ice cap does not develop, and volumes are up to 60 % smaller than ice volumes predicted from the volume-area relation derived from our steady-state experiments (Fig. 13b). Approaching the LIA and up to today, Hardangerjøkulen has a more developed shape, and our steady-state derived volume-area relation fits well with simulated volumes. We discuss these results and their implications in Sect. 5.5.

5 Discussion

5.1 Sensitivity to sliding and deformation parameters

Running our parameter calibration ensemble, we aim to minimize the Root Mean Square Error (RMSE) between observed and modelled present-day surface topography. Several parameter combinations give similar RMSEs (Fig. 3). Since both the rate factor (A) and sliding parameter (β) depend on driving stress (Flowers et al., 2008; Zekollari et al., 2013), one can keep the same surface velocities by reducing one parameter and increasing the other. Hence it is challenging to pick a unique combination without more empirical knowledge about their relative importance (Le Meur and Vincent, 2003; Adalgeirsdóttir et al., 2011; Zekollari et al., 2013). This underlines the motivation behind keeping our ensemble after the calibration. A comparison with an ice velocity map, which is not available for Hardangerjøkulen, would more strongly constrain A and β.

Notwithstanding data deficiencies, a notable finding is that the impact of A on ice volume is relatively small at calibration (Fig. 3), but large during our transient simulation over several centuries (Fig. 4d). This disparity suggests that small differences in model rheology at initialization can propagate significantly with time. This time-dependency has implications for other model studies of long-term dynamics of glaciers and ice caps. With growing availability of data, such studies may consider a

'dynamic' or 'transient' calibration (e.g. Oerlemans, 1997a; Davies et al., 2014; Goldberg et al., 2015), as opposed to a 'snapshot' calibration. The 'transient' method uses several sets of observations to infer model parameters, ideally at dynamically and climatically different states.

During the years following 1600 AD, when including the ensemble of dynamical parameters, the ice cap response is a combined effect of climate forcing and adjustment to new parameter values. The period 1600–1710 AD can be viewed as a short spinup phase for the historic simulation, where the mass balance is kept constant at the end value of the Holocene simulation ($\Delta B(t) = 0.4$ m w.e.).

For the historic run, the ensemble spread in surface elevation is larger in the vicinity of the ELA than at the margins (Fig. 7). Recall that the continuity equation (Eq. 4) requires that thickness change occurs ($\frac{\partial H}{\partial t} \neq 0$) if ice flow and mass balance are not balanced ($\nabla \cdot (\bar{u}H) \neq \dot{M}$). Therefore, softer ice or higher sliding cause ice thickness to decrease, meaning ice spends less time in the accumulation zone. Similarly, faster flow downstream of the ELA also requires thinning. The insensitivity of the frontal positions is likely due to high ablation near the margins overwhelming other effects, and for 1995 also frontal positions pinned by bedrock topography.

Flowers et al. (2008) simulated Holocene behavior of the Langjökull ice cap on Iceland using $\beta = 2.5 \times 10^{-4}$ m a^{-1}Pa^{-1}, which is within our ensemble range. Somewhat in contrast to this study, they noted a low sensitivity to β. However, seasonal speed-ups are absent at Langjökull while they have been observed at Hardangerjøkulen (Willis, 1995; Willis et al., 2012), which probably explains the differing sensitivities.

In line with our study, Hubbard et al. (2006) obtained a shallow, dynamic Icelandic ice sheet at the Last Glacial Maximum, associated with high sliding. Similarly, Golledge et al. (2008) obtained a thin, more extensive Younger Dryas ice sheet in Scotland with increased sliding. As also explained above from a theoretical perspective (mass continuity), a shallow geometry is associated with high sliding.

A future expansion of this work would be a multiple regression of the dynamical parameters for Hardangerjøkulen and its outlet glaciers. This could disentangle whether their importance changes over time, for example depending on mass balance regime or whether the glacier is retreating or advancing. However, the available (velocity) data are not sufficient to constrain the dynamic parameters to a narrower range, thus more data would be needed to make such an analysis insightful. Better knowledge of the bed properties at Hardangerjøkulen by means of radar, seismics or borehole studies, along with modeling of the subglacial drainage system, would also be steps toward understanding the (transient) behavior of basal slipperiness.

5.2 Mass balance parametrization

We deliberately chose to use a simple mass balance formulation, to focus on first order ice dynamical responses to spatially homogeneous changes in the forcing. The evolution of Hardangerjøkulen through the 20th century has been simulated by Giesen (2009) using the simple mass balance profile used here, as well as with a spatially distributed mass and energy balance model (Giesen and Oerlemans, 2010). Differences in ice volume and outlet glacier lengths produced with the two mass balance configurations were present, but small, justifying the use of the simple mass balance profile. In this section, we discuss some of the results presented in Giesen (2009) and Giesen and Oerlemans (2010) that are relevant for our study.

Similar to the present study, Giesen and Oerlemans (2010) were not able to match both the modelled lengths of Rembesdal-skåka and Midtdalsbreen with modern observations. Since they used a sophisticated mass balance model including an albedo scheme, a spatial precipitation gradient, and aspect and shading effects on insolation, this suggests that the mismatch should not be attributed to the mass balance forcing, but to other factors.

5   The two single years (2001-02; Krantz, 2002) with mass balance measurements on Midtdalsbreen are not enough to systematically assess differences in the mass balance regimes of Rembesdalskåka and Midtdalsbreen. Nonetheless, differing mass balance regimes were suggested based on surface elevation changes from 1961 to 1995 (Andreassen and Elvehøy, 2001), and also served as an explanation for differing glacier reconstructions between the southwestern and northeastern margins of the ice cap (Dahl and Nesje, 1994; Nesje et al., 1994). Coupled glacier and precipitation reconstructions based on multiproxy

10 approaches on lacustrine sediments (e.g. Vasskog et al., 2012) could give more insight into differing continentality of the outlet glaciers of Hardangerjøkulen. Snow and mass balance field studies covering the entire ice cap would also be valuable to better understand the spatial mass balance variability.

Apart from spatial variations in the mass balance profile, temporal changes in climate or ice cap geometry may affect the mass balance function. For example, solar insolation patterns may change with strongly altered ice cap geometry, by shading

15 effects of valley walls. However, Hardangerjøkulen has a gently sloping surface and is not surrounded by high mountains. Therefore, topographic effects on the insolation result in small spatial variations of the mass balance between -0.1 and +0.1 m w.e. for the vast majority of the ice cap, only two outlet glaciers oriented south show larger deviations locally. Even in a considerably warmer climate with a smaller ice cap, with continuously updated topographic effects on solar radiation, the mass balance profile with elevation remained close to the present-day value. Furthermore, solar irradiance at 4000 BP, when we start

20 our simulation, was at most 5% larger in the summer months than today (Giesen, 2009), and is therefore expected to have a minor effect on mass balance. In addition, Giesen and Oerlemans (2010) show that lowering the ice albedo from 0.35 to 0.20 under a realistic 21st century scenario only leads to a 5 % larger volume decrease of the ice cap. We conclude that using a mass balance profile only dependent on elevation is a good approximation for Hardangerjøkulen, even in a different climate with a smaller or larger ice cap.

25 It is not clear why *observed* mass balance decreases at the uppermost elevations (Fig. 2), but likely explanations are snow redistribution by wind or orographic precipitation effects. Snow erosion and redeposition may be parametrized based on surface curvature, which is a good indicator of regions with wind-induced snow redistribution (Blöschl et al., 1991; Huss et al., 2008). Giesen (2009) tested a surface-curvature approach for Hardangerjøkulen, however the plateau was too flat for snow redistribution to occur in the model. An orographic precipitation model has not yet been applied to Hardangerjøkulen and is

30 outside the scope of our study.

Glaciological measurements of mass balance have inherent uncertainties and biases, related to instrumentation, survey practices and techniques (Cogley et al., 2011). Andreassen et al. (2015) performed a reanalysis of glaciological and geodetic mass balance for Norwegian glaciers, including Rembesdalskåka. For the period 1995–2010, they found a more negative geodetic mass balance (-0.45 m w.e.) than the glaciological one used in this study. We performed an additional simulation with this

more negative mass balance for the final years of our simulation (1995–2008) and found that the effect on ice volume is c. 0.5 km^3, or 5.3 % of modelled ice volume in year 2008.

5.3   Mass balance sensitivity and hysteresis

Hardangerjøkulen is found to be particularly sensitive to mass balance changes: the ice cap disappears completely for the -0.5 m w.e. anomaly forcing, and almost doubles in volume for +0.5 m w.e. Similar experiments for Nigardsbreen, southwestern Norway (Oerlemans, 1997a), and Franz Josef Glacier, southwestern New Zealand (Oerlemans, 1997b) show much smaller responses (∼20-25 %). Our results are consistent with those of Giesen (2009), who also used a SIA model (Van Den Berg et al., 2008), but with different implementation of dynamical parameters and numerical methods.

Hardangerjøkulen's high sensitivity can be explained by its hypsometry and surface topography. Rivera and Casassa (1999) attributed differing responses of three Patagonian glaciers to contrasting hypsometries and thereby sensitivity to ELA change. Nesje et al. (2008a) noted that the difference between Hardangerjøkulen's ELA and maximum elevation is particularly small (∼180 m) compared to other glaciers and ice caps in Norway. Furthermore, the ice cap is relatively flat with little area distribution in altitude. A comparison with Franz Josef Glacier, New Zealand (Woo and Fitzharris, 1992), Nigardsbreen, Norway (Oerlemans, 1997a), and Vatnajökull, Iceland (Aðalgeirsdóttir et al., 2003) confirms that Hardangerjøkulen's has the most extreme hypsometry (Fig. 14a). Furthermore, the present ELA is located close to the altitudes where area is large, resulting in an unusually vulnerable ice cap. For example, an ELA increase of 100 m at Hardangerjøkulen is equivalent to a 16.9 % decrease in area. Corresponding values for Nigardsbreen (9.9 %), Franz Josef Glacier (1.5 %) and Vatnajökull (6.1 %) are much smaller, confirming this explanation (Fig. 14b).

The high sensitivity to mass balance changes found for Hardangerjøkulen supports abrupt changes inferred from lake sediment records for the Holocene for both the northern and southern side of the ice cap (Dahl and Nesje, 1994; Nesje et al., 1994). One example is the so called *Finse event*, when an advance to a maximum extent beyond that of present-day of the northern Blåisen outlet glacier ∼8300 BP was followed by a complete disappearance of this glacier within less than a century. Our results show that for a mass balance anomaly of -0.5 m w.e., the present-day ice cap disappears in ∼300 years. Depending on the ice cap volume at the Finse event, we find that an anomaly between -2.0 to 2.4 m w.e. melts away Hardangerjøkulen within a century. Nonetheless, the advanced ice cap at the Finse event was likely not fully grown and in a steady-state, so an anomaly of ∼1.5 m w.e. is more likely.

Given a mass balance sensitivity of around -0.9 m w.e. K^{-1} (Giesen and Oerlemans, 2010) and no change in precipitation, the air temperature increase responsible for the ice cap disappearance after the Finse event must have been at least 1.5 K. Reconstructed summer temperature after the Finse event suggest a sharp increase of 1.0-1.2 K (Dahl and Nesje, 1996). A 10 % precipitation decrease would compensate for this difference, since the sensitivity to precipitation for Hardangerjøkulen is around +0.3 m w.e. K^{-1} (Giesen and Oerlemans, 2010). Despite uncertainties in the reconstruction and model simulations, it is encouraging that both give consistent results, suggesting that ice flow models coupled with reconstructions may be used to constrain past climate conditions.

We can also view our results on mass balance sensitivity in light of future climate change. The mean mass balance in the last decade was -0.3 m w.e. Since Hardangerjøkulen was in approximate balance over the preceding decades, this decrease primarily reflects changes in meteorological conditions, and not dynamical adjustments. With the mass balance of the last decade, our experiments suggest that Hardangerjøkulen disappears within 750 years (Fig. 11). However, future projections indicate further warming for southern Norway. Giesen and Oerlemans (2010) imposed future climate scenarios on a surface energy balance mass balance model coupled to a SIA model, suggesting that Hardangerjøkulen will vanish almost completely before 2100. Similar conclusions have been reached for glaciers in Iceland (Adalgeirsdóttir et al., 2006; Guðmundsson et al., 2009; Adalgeirsdóttir et al., 2011), French Alps (Le Meur et al., 2007), Swiss Alps (Jouvet et al., 2011) and Canadian Rocky Mountains (Clarke et al., 2015). Given the aforementioned temperature and precipitation sensitivities for Hardangerjøkulen, our estimate of -2.2 m w.e. to remove the present-day ice cap in 100 years translates to a temperature increase of ∼2.7 °C, given a 10 % increase in precipitation. This is close to future projections for southern Norway (Hansen-Bauer et al., 2015).

Hardangerjøkulen's strong hysteresis highlights the importance of accurately representing the initial state in transient simulations of small ice caps, as previously suggested for ice sheets (e.g Aschwanden et al., 2013; Aðalgeirsdóttir et al., 2014). Starting from ice-free conditions, Hardangerjøkulen grows to only 20% of its present-day volume under a modern climate. This is in stark contrast to the Juneau Icefield in Alaska, an ice field in a similar climatic setting, which in model simulations regrows close to modern ice volume under present-day mass balance conditions (Ziemen et al., 2016). The authors attribute this insensitivity to initial conditions to the complex topography of the Juneau Icefield, with numerous outlet glaciers able to retreat up to high altitudes where positive mass balance areas persist even under future warming scenarios. This behavior is not observed at Yakutat Icefield, a low-lying maritime ice field in southeast Alaska (Trüssel et al., 2015), which cannot be sustained under present-day climate conditions. Its topography is relatively flat, comparable to the one of Hardangerjøkulen, which might explain its high sensitivity under modern climate scenarios. Similarly, Gilbert et al. (2016) suggested that Barnes Ice Cap, Baffin Island, Canada, is not sustainable under present mass balance conditions. While they did not perform regrowth experiments, their findings of the Barnes Ice Cap being a remnant of the Laurentide Ice Sheet suggest a hysteresis similar as we show for Hardangerjøkulen.

5.4 Holocene to LIA build-up

In the early part of the modelled period (c. 4000 - 3800 BP), ice grows preferentially on high bed topography, and Midtdalsbreen and Blåisen start to develop earlier than Rembesdalskåka (Fig. 5, also see Fig. 1). While the model resolution here is coarse (300-500 m), we expect that ice dynamics at this stage plays a minor role, since the ice present is split up into several small separate glaciers (< 2 km long, < 100 m thick). Instead, the initial ice growth at high bed ridges is due to build-up of ice above the present-day ELA, which is used as initial mass balance forcing.

The actual rate of advance may differ from what is modelled here because the SIA has limitations in the steep terrain (Le Meur et al., 2004) where Rembesdalskåka terminates during the period of fast ice volume increase (c. 3800–2300 BP, Fig. 4c). However, the effects of ice flow mechanics are likely small compared to those of the mass balance on the long time scales considered here.

During the period of modelled rapid ice cap growth (c. 2300–1300 BP), reconstructed precipitation in western Norway is slightly lower than the general increasing mass balance trend applied here (Dahl and Nesje, 1996; Bjune et al., 2005). At the same time, glacier reconstructions from southern Hardangerjøkulen indicate a slight decrease in glacier size (Nesje et al., 1994). Unfortunately, there is to our knowledge no geomorphological or other evidence that can be used as tie points for modelled ice cap extent or volume during this period.

Our simulated preferential ice cap growth on the northern and western side, illustrated in Fig. 5b at 2300 BP, is in line with reconstructions showing an early glacierization of the north (Dahl and Nesje, 1994) versus the south (Nesje et al., 1994).

We are aware that bed topography for Hardangerjøkulen is uncertain in places, though less so for Midtdalsbreen and Rembesdalskåka, which are of prime interest. Moreover, the proglacial lake in front of Rembesdalskåka may have modulated LIA frontal behavior, as suggested for Icelandic glaciers (Hannesdóttir et al., 2015). We however expect this effect to be minor compared to other model uncertainties.

Further data for model validation is required to add more detail to our modelled history of Hardangerjøkulen. However, given the limited knowledge about ice cap activity between the ice-free conditions at 4000 BP and the LIA maximum around 1750 AD, we consider our continuous model simulation to be a good first estimate of Hardangerjøkulen's growth from inception to its maximum extent during the LIA.

Moreover, we have provided a plausible ice cap history over several thousand years as the starting point for our simulations from the LIA until today, in contrast to several previous studies (e.g. Giesen and Oerlemans, 2010; Adalgeirsdóttir et al., 2011; Zekollari et al., 2014) reaching desired initial LIA conditions by perturbing a present-day ice cap.

5.5 Non-linearity, asymmetry and their implications

The initial present-day mass balance forcing ($\Delta B(t) = 0$ m w.e.) at 4000 BP likely explains the rapid increase in ice volume over the first few hundred years, since this forcing essentially represents a step change in mass balance at 4000 BP. However, this effect diminishes after a few hundred years, after which the response is due to the linear mass balance forcing. $\Delta B(t) = 0$ m w.e. starting from ice-free conditions produces a steady-state ice volume of only ~ 2 km^3 (Fig. 10), a volume exceeded at 3300 BP, so any additional ice volume cannot be explained by the initial step change in mass balance at 4000 BP. Most importantly, the non-linear ice volume response between 2300–1300 BP is thus entirely forced by the linear mass balance increase during this period.

Analogous to the Holocene simulations, we performed experiments with a slowly *decreasing* mass balance over multiple millennia (from $\Delta B(t) = 0.4$ to 0 m w.e.), allowing the ice cap to dynamically adjust, starting with the 1600 AD ice cap state. We find that the western ice cap disappears first, while ice in the eastern part of the ice cap is more persistent. Hence, the western and northern parts of the ice cap grow first and disappear first, whereas the eastern part grows last and disappears last. Further, our experiments show that a gradual (linear) climatic change results in a non-linear change in ice volume. This non-linear, asynchronous growth and retreat illustrates that proxy records representing different parts of an ice cap at different times may lead to substantially different conclusions about ice cap size through time.

Previous work has highlighted glacier hypsometry, overdeepenings and proglacial lakes in altering glacier *retreat* to climate forcing (Kuhn et al., 1985; Jiskoot et al., 2009; Adalgeirsdóttir et al., 2011). Adhikari and Marshall (2013) and Hannesdóttir et al. (2015) showed that overdeepened basins loose mass by thinning rather than retreat. Here we suggest that a similar behavior applies to an *advancing* glacier. In particular, overdeepened areas delay frontal advance and lead to preferential

5   glacier thickening. However, note that the effect of higher order stresses, not captured by our simplified dynamic model, may be more important for an advancing glacier (Adhikari and Marshall, 2013).

Regarding volume-area scaling (Sect. 4.4), Bahr et al. (2015) argues that the fundamental difference between valley glaciers and ice caps, and hence the reason for different scaling exponents (γ), is the influence of bedrock topography, specifically that ice thickness is large compared to the relief of underlying topography. The bedrock topography below Hardangerjøkulen

10   consists of deep subglacial valleys and high ridges controlling the ice flow, as also noted by Laumann and Nesje (2016) for other Norwegian ice caps. In fact, our simulations confirm that bed topography is vital in controlling the growth and retreat of Hardangerjøkulen. The relatively thin ice at the ice cap summit does not correspond to the classical ice cap with the thickest ice in the center, which explains why volume-area exponents for valley glaciers ($\gamma = 1.375$) rather than ice caps ($\gamma = 1.25$) are found for Hardangerjøkulen. However, the overestimation of c by commonly used volume-area scaling relations for ice caps

15   is more surprising. The low c we find compared to literature values for ice caps suggests that literature volume-area scaling parameters may not be accurate for relatively small ice caps.

Importantly, glacier reconstructions using proglacial lake sediments are generally based on assumed changes in glacier (erosive) area rather than volume (Hallet et al., 1996), while we show that volume and area can become decoupled for several centuries (Fig. 12). We also demonstrate that the degree of volume-area coupling varies for different outlet glaciers, implying

20   that each outlet glacier should be considered individually. For example, a differing response to identical climate forcing is illustrated when Midtdalsbreen advances only modestly from 2300–1300 BP (Fig. 5b-d), while Hardangerjøkulen triples its ice volume during the same period due to ice growth elsewhere (mainly in the east, south and southwest).

Our non-linear response and out-of-phase volume and area calls for reassessment of some glacier and climate reconstruction methodologies. To extract a climate signal, linear assumptions between ice extent (area), ice volume (mass balance), climate,

25   and their geomorphological or proxy signal are commonly assumed in glacier reconstructions (e.g. Liestøl in Sissons, 1979; Bakke et al., 2005). Linearity is also commonly assumed in simplified models used to extract climate information from glacier variations (e.g Harrison et al., 2001; Oerlemans, 2005; Lüthi, 2009; Roe, 2011). However, we find that these assumptions do not hold for Hardangerjøkulen and its outlet glaciers. For a growing ice cap, two scenarios may arise for which the linear assumption between area (proxy) and volume (climate) fails: (i) area changes faster than volume (first few hundred years

30   of our Holocene simulation), meaning the interpreted signal becomes biased towards a climate favorable for glacier growth (wetter/colder), or (ii) volume changes faster than area (2300–1300 BP in our simulation), and the climate signal is missed or underestimated because the preferential thickening is not translated into a corresponding frontal change. We expect that ice caps with comparable geometry in for example Norway, Iceland, Alaska, Patagonia and peripheral Greenland may display similar behavior.

These results highlight the need for model-data integration in paleostudies. Ice sheet modelers require glacier records for calibration and validation, and climate reconstructions for model forcing. Based on our experiments, we advise that glacier-derived climate records are tagged with explicitly stated glaciological assumptions and associated uncertainties. In particular, we would like to recommend future model-data studies which directly constrain geometric contributions to the glaciological uncertainties involved in sedimentary glacier proxies.

6 Conclusions

We have used a two-dimensional ice flow model with a simple mass balance parametrization to simulate the evolution of Hardangerjøkulen ice cap since the mid-Holocene, from ice-free conditions up to the present-day. Until the LIA, the model is forced by a linear mass balance increase based on reconstructions of temperature and precipitation. From the LIA onwards, an optimized mass balance history is employed, and direct mass balance measurements are used after 1963.

We used an ensemble approach to assess sensitivity to sliding and ice deformation parameters during both calibration and transient runs. We find that small differences in model ice rheology at the calibration stage increase significantly with time. This time-dependence has implications for other model studies of long-term dynamics of glaciers and ice caps. Such studies would benefit from using a 'transient calibration' rather than a 'snapshot' approach, and thereby reduce temporal biases arising from data quality issues, or a particular dynamic or climatic state. More data in both space and time is needed to further constrain the dynamic model parameters and mass balance for Hardangerjøkulen.

In our simulations, Hardangerjøkulen evolves from no ice in the mid-Holocene to its LIA maximum in different stages, where the fastest stage (2200–1300 BP) involves a tripling of ice volume in less than 1000 years. Notably, our linear climate forcing during this time gives a non-linear response in ice cap volume and area. This growth occurs in a spatially asymmetric fashion, where Midtdalsbreen reaches its maximum first, while advances of Rembesdalskåka and the eastern ice cap are delayed. These different responses are caused by local bed topography and the mass balance-altitude feedback.

Following the simulated Holocene growth of Hardangerjøkulen, we successfully reproduce the main features of the LIA extent of the main outlet glaciers, given temporal and spatial uncertainties in moraine evidence. In the early 1900s the simulated glacier positions are slightly underestimated, whereas the ice extent closely resembles the observed margins available starting from 1960, and the surface topography fits well with the 1995 surface survey.

Hardangerjøkulen is found to be highly sensitive to mass balance changes. A reduction by 0.2 m w.e. or more relative to the mass balance from the last decades induces a strong mass balance-altitude feedback and makes the ice cap disappear completely. Conversely, an anomaly of +0.5 m w.e. almost doubles total ice volume.

Volume and area for Hardangerjøkulen and several of its outlet glaciers vary out-of-phase for several centuries during the Holocene. This disequilibrium varies in time and among the outlet glaciers, showing that ice cap reconstruction methodologies carrying linear assumptions between ice extent and volume may not hold. Based on the non-linear, asynchronous response we find for Hardangerjøkulen, these paleoglaciological studies may decrease their uncertainty by (i) quantifying the effect of bedrock topography on ice flow and mass balance, using a numerical model; (ii) performing reconstructions on at least two

outlet glaciers, preferably with distinct dynamics and bedrock topography, and (iii) reporting glaciological assumptions and proxy uncertainties to ice sheet modelers using their data.

Our experiments suggest that the present-day ice cap is in a mass balance regime where it will not regrow once it has disappeared. We thus find that Hardangerjøkulen displays strong hysteresis and that the interaction between hypsometry and mass balance-altitude feedback controls its behavior. By combining our modelled sensitivities with past climatic and glacier information, we also illustrate that ice flow models can further constrain past climates and glacier states. This highlights the need to understand the long-term history of glaciers and ice caps and calls for further integrated model-data studies.

Acknowledgements. We wish to acknowledge NVE for access to mass balance data, glacier outlines, and surface and bed DEMs. Thanks also to Norwegian Meteorological Institute for providing climate data (eklima.no). We are also grateful to Atle Nesje for sharing detailed knowledge about Hardangerjøkulen, and for reading the manuscript prior to submission. The research leading to these results has received funding from the European Research Council under the European Community's Seventh Framework Programme (FP7/2007-2013) / ERC grant agreement 610055 as part of the ice2ice project. This research is also supported by the Research Council of Norway via the NOTUR project NN4659K "Models of past ice and climate". HÅ was supported by the Research Council of Norway (project no. 229788/E10), as part of the research project Eurasian Ice Sheet and Climate Interactions (EISCLIM), and has also received travel support from BKK AS. HÅ, KHN, RG and MM designed the research, HÅ performed the model runs with significant input from KHN and RG, MM provided the ice sheet model and added necessary implementations together with HÅ. HÅ created all figures and wrote the paper, with substantial contributions from all the authors. We wish to thank Andy Aschwanden, Nicholas R. Golledge, two anonymous reviewers and the Editor Andreas Vieli, whose thorough comments greatly improved the original manuscript. The authors declare that they have no conflict of interest.

References

Aðalgeirsdóttir, G., Gudmundsson, G. H., and Björnsson, H.: A regression model for the mass-balance distribution of the Vatnajo̊ kull ice cap, Iceland, Annals of Glaciology, 37, 189–193, 2003.

Aðalgeirsdóttir, G., Aschwanden, A., Khroulev, C., Boberg, F., Mottram, R., Lucas-Picher, P., and Christensen, J.: Role of model initialization for projections of 21st-century Greenland ice sheet mass loss, Journal of Glaciology, 60, 782–794, 2014.

Adalgeirsdóttir, G., Jóhannesson, T., Björnsson, H., Pálsson, F., and Sigurðsson, O.: Response of Hofsjökull and southern Vatnajökull, Iceland, to climate change, Journal of Geophysical Research: Earth Surface (2003–2012), 111, doi:10.1029/2005JF000388, 2006.

Adalgeirsdóttir, G., Guðmundsson, S., Björnsson, H., Pálsson, F., Jóhannesson, T., Hannesdóttir, H., Sigurdsson, S., Berthier, E., et al.: Modelling the 20th and 21st century evolution of Hoffellsjökull glacier, SE-Vatnajökull, Iceland, The Cryosphere, 5, 961–975, doi:dx.doi.org/10.5194/tc-5-961-2011, 2011.

Adhikari, S. and Marshall, S.: Influence of high-order mechanics on simulation of glacier response to climate change: insights from Haig Glacier, Canadian Rocky Mountains., Cryosphere, 7, doi:dx.doi.org/10.5194/tc-7-1527-2013, 2013.

Andersen, J. and Sollid, J.: Glacial chronology and glacial geomorphology in the marginal zones of the glaciers, Midtdalsbreen and Nigardsbreen, south Norway, Norsk Geografisk Tidskrift, 25, 1–38, 1971.

Andreassen, L. and Elvehøy, H.: Volume change - Hardangerjøkulen, chap. Glaciological investigations in Norway in 2000, pp. 101–102, NVE Report No 2. Norwegian Water Resources and Energy Directorate, Oslo, 2001.

Andreassen, L., Elvehøy, H., and Kjøllmoen, B.: Laser scanning of Norwegian mass balance glaciers 2007-2011, in: EGU General Assembly Conference Abstracts, vol. 14, p. 10941, http://ncoe-svali.org/xpdf/andreassen_et_al_egu2012.pdf, 2012.

Andreassen, L. M., Elvehøy, H., Kjøllmoen, B., Engeset, R. V., and Haakensen, N.: Glacier mass-balance and length variation in Norway, Annals of Glaciology, 42, 317–325, 2005.

Andreassen, L. M., Elvehøy, H., Kjøllmoen, B., and Engeset, R. V.: Glaciological and geodetic mass balance of ten long-term glaciers in Norway, The Cryosphere Discussions, 9, 6581–6626, doi:10.5194/tcd-9-6581-2015, 2015.

Arendt, A., Bliss, A., Bolch, T., Cogley, J., Gardner, A., Hagen, J.-O., Hock, R., Huss, M., Kaser, G., Kienholz, C., Pfeffer, W., Moholdt, G., Paul, F., Radic, V., Andreassen, L., Bajracharya, S., Barrand, N., Beedle, M., Berthier, E., Bhambri, R., Brown, I., Burgess, E., Burgess, D., Cawkwell, F., Chinn, T., Copland, L., Davies, B., De Angelis, H., Dolgova, E., Earl, L., Filbert, K., Forester, R., Fountain, A., Frey, H., Giffen, B., Glasser, N., Guo, W., Gurney, W., Hagg, W., Hall, D., Haritashya, U., Hartmann, G., Helm, C., Herreid, S., Howat, I., Kapustin, G., Khromova, T., König, M., Kohler, J., Kriegel, D., Kutuzov, S., Lavrentiev, I., LeBris, R., Liu, S., Lund, J., Manley, W., Marti, R., Mayer, C., Miles, E., Li, X., Menounos, B., Mercer, A., Mölg, N., Mool, P., Nosenko, G., Negrete, A., Nuimura, T., Nuth, C., Pettersson, R., Racoviteanu, A., Ranzi, R., Rastner, P., Bau, F., Raup, B., Rich, J., Rott, H., Sakai, A., Schneider, C., Seliverstov, Y., Sharp, M., Sigurdsson, O., Stokes, C., Way, R., Wheate, R., Winsvold, S., Wolken, G., Wyatt, F., and Zheltyhina, N.: Randolph Glacier Inventory - A Dataset of Global Glacier Outlines: Version 5.0, Glims technical report, Global Land Ice Measurements from Space, 2015.

Aschwanden, A., Aðalgeirsdóttir, G., and Khroulev, C.: Hindcasting to measure ice sheet model sensitivity to initial states, The Cryosphere, 7, 1083–1093, 2013.

Bahr, D. B., Meier, M. F., and Peckham, S. D.: The physical basis of glacier volume-area scaling, Journal of Geophysical Research, 102, 20 355, 1997.

Bahr, D. B., Pfeffer, W. T., and Kaser, G.: A review of volume-area scaling of glaciers, Reviews of Geophysics, 53, 95–140, 2015.

Bakke, J., Øivind, L., Nesje, A., Dahl, S. O., and Paasche, Ø.: Utilizing physical sediment variability in glacier-fed lakes for continuous glacier reconstructions during the Holocene, northern Folgefonna, western Norway, The Holocene, 15, 161–176, doi:10.1191/0959683605hl797rp, 2005.

Berthier, E., Schiefer, E., Clarke, G. K., Menounos, B., and Rémy, F.: Contribution of Alaskan glaciers to sea-level rise derived from satellite imagery, Nature Geoscience, 3, 92–95, 2010.

Bjune, A. E., Bakke, J., Nesje, A., and Birks, H. J. B.: Holocene mean July temperature and winter precipitation in western Norvay inferred from palynological and glaciological lake-sediment proxies, The Holocene, 15, 177–189, 10.1191/0959683605hl798rp, 2005.

Blöschl, G., Kirnbauer, R., and Gutknecht, D.: Distributed snowmelt simulations in an alpine catchment: 1. Model evaluation on the basis of snow cover patterns, Water Resources Research, 27, 3171–3179, doi:10.1029/91WR02250, 1991.

Church, J., Clark, P., Cazenave, A., Gregory, J., Jevrejeva, S., Levermann, A., Merrifield, M., Milne, G., Nerem, R., Nunn, P., Payne, A., Pfeffer, W., Stammer, D., and Unnikrishnan, A.: Sea Level Change, chap. Climate Change 2013: The Physical Science Basis. Contribution of Working Group I to the Fifth Assessment Report of the Intergovernmental Panel on Climate Change, Cambridge University Press, Cambridge, United Kingdom and New York, NY, USA, 2013.

Clarke, G. K., Jarosch, A. H., Anslow, F. S., Radić, V., and Menounos, B.: Projected deglaciation of western Canada in the twenty-first century, Nature Geoscience, 8, 372–377, doi:10.1038/ngeo2407, 2015.

Cogley, J., Hock, R., Rasmussen, L., Arendt, A., Bauder, A., Braithwaite, R., Jansson, P., Kaser, G., Möller, M., Nicholson, L., et al.: Glossary of glacier mass balance and related terms, IHP-VII technical documents in hydrology No. 86, IACS Contribution No. 2, 2011.

Cuffey, K. M. and Paterson, W. S. B.: The physics of glaciers, Elsevier, 2010.

Dahl, S. O. and Nesje, A.: Holocene glacier fluctuations at Hardangerjøkulen, central-southern Norway: a high-resolution composite chronology from lacustrine and terrestrial deposits, The Holocene, 4, 269–277, doi:10.1177/095968369400400306, 1994.

Dahl, S. O. and Nesje, A.: A new approach to calculating Holocene winter precipitation by combining glacier equilibrium-line altitudes and pine-tree limits: a case study from Hardangerjøkulen, central southern Norway, The Holocene, 6, 381–398, doi:10.1177/095968369600600401, 1996.

Davies, B. J., Golledge, N. R., Glasser, N. F., Carrivick, J. L., Ligtenberg, S. R., Barrand, N. E., Van Den Broeke, M. R., Hambrey, M. J., and Smellie, J. L.: Modelled glacier response to centennial temperature and precipitation trends on the Antarctic Peninsula, Nature Climate Change, 4, 993–998, 2014.

Elvehøy, H., Kohler, J., Engeset, R., and Andreassen, L.: Jøkullaup fra Demmevatn, NVE Report 17, 1997.

Flowers, G. E., Björnsson, H., Geirsdóttir, Á., Miller, G. H., Black, J. L., and Clarke, G. K.: Holocene climate conditions and glacier variation in central Iceland from physical modelling and empirical evidence, Quaternary Science Reviews, 27, 797–813, doi:10.1016/j.quascirev.2007.12.004, 2008.

Giesen, R.: The ice cap Hardangerjøkulen in the past, present and future climate, Ph.D. thesis, IMAU, Utrecht University, 2009.

Giesen, R. and Oerlemans, J.: Response of the ice cap Hardangerjøkulen in southern Norway to the 20th and 21st century climates, The Cryosphere, 4, 191–213, doi:10.5194/tc-4-191-2010, 2010.

Gilbert, A., Flowers, G. E., Miller, G. H., Rabus, B. T., Van Wychen, W., Gardner, A. S., and Copland, L.: Sensitivity of Barnes Ice Cap, Baffin Island, Canada, to climate state and internal dynamics, Journal of Geophysical Research: Earth Surface, 121, 1516–1539, doi:10.1002/2016JF003839, 2016.

Glen, J. W.: The creep of polycrystalline ice, Proceedings of the Royal Society of London. Series A. Mathematical and Physical Sciences, 228, 519–538, doi:10.1098/rspa.1955.0066, 1955.

Goldberg, D., Heimbach, P., Joughin, I., and Smith, B.: Committed retreat of Smith, Pope, and Kohler Glaciers over the next 30 years inferred by transient model calibration, The Cryosphere, 9, 2429–2446, 2015.

Golledge, N. R., Hubbard, A., and Sugden, D. E.: High-resolution numerical simulation of Younger Dryas glaciation in Scotland, Quaternary Science Reviews, 27, 888–904, doi:10.1016/j.quascirev.2008.01.019, 2008.

Greve, R. and Blatter, H.: Dynamics of ice sheets and glaciers, Springer, 2009.

Grinsted, A.: An estimate of global glacier volume, The Cryosphere, 7, 141–151, 2013.

Gudmundsson, G. H.: Transmission of basal variability to a glacier surface, Journal of Geophysical Research: Solid Earth (1978–2012), 108, doi:10.1029/2002JB002107, 2003.

Guðmundsson, S., Björnsson, H., Jóhannesson, T., Adalgeirsdóttir, G., Pálsson, F., and Sigurðsson, O.: Similarities and differences in the response to climate warming of two ice caps in Iceland., Hydrology Research, 40, doi:10.2166/nh.2009.210, 2009.

Hagen, J. O.: Brefrontprosesser ved Hardangerjøkulen (Glacial terminus processes at Hardangerjøkulen)., Ph.D. thesis, Department of Geography. University of Oslo, Norway, 1978.

Hallet, B., Hunter, L., and Bogen, J.: Rates of erosion and sediment evacuation by glaciers: A review of field data and their implications, Global and Planetary Change, 12, 213–235, doi:10.1016/0921-8181(95)00021-6, 1996.

Hannesdóttir, H., Björnsson, H., Pálsson, F., Aðalgeirsdóttir, G., and Guðmundsson, S.: Changes in the southeast Vatnajökull ice cap, Iceland, between˜ 1890 and 2010, The Cryosphere, 9, 565–585, doi:10.5194/tc-9-565-2015, 2015.

Hansen-Bauer, I., Førland, E., Haddeland, I., Hisdal, H., Mayer, S., Nesje, A., Nilsen, J., Sandven, S., Sandø, A., Sorteberg, A., et al.: Klima i Norge 2100 Kunnskapsgrunnlag for klimatilpasning oppdatert i 2015, NCCS report, Oslo, Norway, p. 203, 2015.

Harrison, W., Elsberg, D., Echelmeyer, K., and Krimmel, R.: On the characterization of glacier response by a single time-scale, Journal of Glaciology, 47, 659–664, doi:10.3189/172756501781831837, 2001.

Hecht, F.: BAMG: Bi-dimensional anisotropic mesh generator, Tech. rep., Inria, St. Ismier, France., 2006.

Hindmarsh, R.: A numerical comparison of approximations to the Stokes equations used in ice sheet and glacier modeling, Journal of Geophysical Research: Earth Surface (2003–2012), 109, doi:10.1029/2003JF000065, 2004.

Hubbard, A., Sugden, D., Dugmore, A., Norddahl, H., and Pétursson, H. G.: A modelling insight into the Icelandic Last Glacial Maximum ice sheet, Quaternary Science Reviews, 25, 2283–2296, doi:10.1016/j.quascirev.2006.04.001, 2006.

Huss, M. and Hock, R.: A new model for global glacier change and sea-level rise, Frontiers in Earth Science, 3, 54, 2015.

Huss, M., Bauder, A., Funk, M., and Hock, R.: Determination of the seasonal mass balance of four Alpine glaciers since 1865, Journal of Geophysical Research: Earth Surface (2003–2012), 113, doi:10.1029/2007JF000803, 2008.

Hutter, K.: Theoretical glaciology: material science of ice and the mechanics of glaciers and ice sheets, Reidel, 1983.

Innes, J. L.: Dating exposed rock surfaces in the Arctic by lichenometry: the problem of thallus circularity and its effect on measurement errors, Arctic, 39, 253–259, 1986.

Jacob, T., Wahr, J., Pfeffer, W. T., and Swenson, S.: Recent contributions of glaciers and ice caps to sea level rise, Nature, 482, 514–518, 2012.

Jiskoot, H., Curran, C. J., Tessler, D. L., and Shenton, L. R.: Changes in Clemenceau Icefield and Chaba Group glaciers, Canada, related to hypsometry, tributary detachment, length–slope and area–aspect relations, Annals of Glaciology, 50, 133–143, doi:10.3189/172756410790595796, 2009.

Jouvet, G., Huss, M., Blatter, H., Picasso, M., and Rappaz, J.: Numerical simulation of Rhonegletscher from 1874 to 2100, Journal of Computational Physics, 228, 6426–6439, 2009.

Jouvet, G., Huss, M., Funk, M., and Blatter, H.: Modelling the retreat of Grosser Aletschgletscher, Switzerland, in a changing climate, Journal of Glaciology, 57, 1033–1045, doi:10.3189/002214311798843359, 2011.

Kalela-Brundin, M.: Climatic information from tree-rings of Pinus sylvestris L. and a reconstruction of summer temperatures back to AD 1500 in Femundsmarka, eastern Norway, using partial least squares regression (PLS) analysis, The Holocene, 9, 59–77, doi:10.1191/095968399678118795, 1999.

Kirchner, N., Ahlkrona, J., Gowan, E. J., Lötstedt, P., Lea, J. M., Noormets, R., von Sydow, L., Dowdeswell, J. A., and Benham, T.: Shallow ice approximation, second order shallow ice approximation, and full Stokes models: A discussion of their roles in palaeo-ice sheet modelling and development, Quaternary Science Reviews, 135, 103–114, 2016.

Kjøllmoen, B., Andreassen, L. M., Elvehøy, H., Jackson, M., Giesen, R. H., and Winkler, S.: Glaciological investigations in Norway in 2010, NVE Report No 3, Norwegian Water Resources and Energy Directorate, Oslo, pp. 1–91, 2011.

Konnestad, H.: Moreneformer i fronten av Midtdalsbreen - en glasiologisk og geomorfologisk undersøkelse av dannelsesprosessene (Moraine formation at the terminus of Midtdalsbreen - a glacial and geomorphological study of their creation), Ph.D. thesis, Department of Geography. University of Oslo, Norway., 1996.

Krantz, K.: Volume changes and traditional mass balance on two outlet glaciers at Hardangerjøkulen, Norway, Master's thesis, Masters thesis unpublished. Department of Geography. University of Oslo, Norway, 2002.

Kuhn, M., Markl, G., Kaser, G., Nickus, U., Obleitner, F., and Schneider, H.: Fluctuations of climate and mass balance: different responses of two adjacent glaciers, Zeitschrift für Gletscherkunde und Glazialgeologie, 21, 409–416, 1985.

Larour, E., Seroussi, H., Morlighem, M., and Rignot, E.: Continental scale, high order, high spatial resolution, ice sheet modeling using the Ice Sheet System Model (ISSM), Journal of Geophysical Research: Earth Surface (2003–2012), 117, doi:0.1029/2011JF002140, 2012.

Laumann, T. and Nesje, A.: Spørteggbreen, western Norway, in the past, present and future: Simulations with a two-dimensional dynamical glacier model, The Holocene, doi:10.1177/0959683614530446, 2014.

Laumann, T. and Nesje, A.: Volume–area scaling parameterisation of Norwegian ice caps: A comparison of different approaches, The Holocene, p. 0959683616652712, 2016.

Le Meur, E. and Vincent, C.: A two-dimensional shallow ice-flow model of Glacier de Saint-Sorlin, France, Journal of Glaciology, 49, 527–538, doi:10.3189/172756503781830421, 2003.

Le Meur, E., Gagliardini, O., Zwinger, T., and Ruokolainen, J.: Glacier flow modelling: a comparison of the Shallow Ice Approximation and the full-Stokes solution, Comptes Rendus Physique, 5, 709–722, doi:10.1016/j.crhy.2004.10.001, 2004.

Le Meur, E., Gerbaux, M., Schäfer, M., and Vincent, C.: Disappearance of an Alpine glacier over the 21st Century simulated from modeling its future surface mass balance, Earth and Planetary Science Letters, 261, 367–374, doi:10.1016/j.epsl.2007.07.022, 2007.

Leysinger-Vieli, G.-M. and Gudmundsson, G.: On estimating length fluctuations of glaciers caused by changes in climatic forcing, Journal of geophysical research, 109, F01 007, doi:10.1029/2003JF000027, 2004.

Lüthi, M. P.: Transient response of idealized glaciers to climate variations, Journal of Glaciology, 55, 918–930, 2009.

MacAyeal, D. R.: A tutorial on the use of control methods in ice-sheet modeling, J. Glaciol, 39, 91–98, 1993.

Melvold, K. and Schuler, T.: Mapping of subglacial topography using GPR for determining subglacial hydraulic conditions, chap. 14, Applied Geophysics in periglacial environments, Cambridge University Press, 2008.

Morland, L.: Thermomechanical balances of ice sheet flows, Geophysical & Astrophysical Fluid Dynamics, 29, 237–266, doi:10.1080/03091928408248191, 1984.

Morlighem, M., Rignot, E., Seroussi, H., Larour, E., Ben Dhia, H., and Aubry, D.: Spatial patterns of basal drag inferred using control methods from a full-Stokes and simpler models for Pine Island Glacier, West Antarctica, Geophysical Research Letters, 37, doi:10.1029/2010GL043853, 2010.

Morlighem, M., Rignot, E., Seroussi, H., Larour, E., Ben Dhia, H., and Aubry, D.: A mass conservation approach for mapping glacier ice thickness, Geophysical Research Letters, 38, doi:10.1029/2011GL048659, 2011.

Nesje, A.: Latest Pleistocene and Holocene alpine glacier fluctuations in Scandinavia, Quaternary Science Reviews, 28, 2119–2136, doi:10.1016/j.quascirev.2008.12.016, 2009.

Nesje, A. and Dahl, S. O.: Holocene glacier variations of Blåisen, Hardangerjøkulen, central southern Norway, Quaternary Research, 35, 25–40, doi:10.1016/0033-5894(91)90092-J, 1991.

Nesje, A. and Dahl, S. O.: The Little Ice Age - only temperature?, The Holocene, 13, 139–145, doi:10.1191/0959683603hl603fa, 2003.

Nesje, A., Dahl, S. O., Løvlie, R., and Sulebak, J. R.: Holocene glacier activity at the southwestern part of Hardangerjøkulen, central-southern Norway: evidence from lacustrine sediments, The Holocene, 4, 377–382, doi:10.1177/095968369400400405, 1994.

Nesje, A., Bakke, J., Dahl, S. O., Lie, Ø., and Matthews, J. A.: Norwegian mountain glaciers in the past, present and future, Global and Planetary Change, 60, 10–27, 2008a.

Nesje, A., Dahl, S., Thun, T., and Nordli, Ø.: The Little Ice Age glacial expansion in western Scandinavia: summer temperature or winter precipitation?, Climate Dynamics, 30, 789–801, doi:10.1007/s00382-007-0324-z, 2008b.

Nordli, P., Lie, Ø., Nesje, A., and Dahl, S. O.: Spring-summer temperature reconstruction in western Norway 1734-2003: a data-synthesis approach, International Journal of Climatology, 23, 1821–1841, doi:10.1002/joc.980, 2003.

Oerlemans, J.: A flowline model for Nigardsbreen, Norway: projection of future glacier length based on dynamic calibration with the historic record, Journal of glaciology, 24, 382–389, 1997a.

Oerlemans, J.: Climate sensitivity of Franz Josef Glacier, New Zealand, as revealed by numerical modeling, Arctic and Alpine Research, pp. 233–239, doi:10.2307/1552052, 1997b.

Oerlemans, J.: Glaciers and climate change, CRC Press, 2001.

Oerlemans, J.: Extracting a climate signal from 169 glacier records, Science, 308, 675–677, 2005.

Østen, K.: Radio-ekko undersøkelser på Midtdalsbreen, Sør-Norge. Master's thesis unpublished., Master's thesis, Department of Geography. University of Oslo, Norway, 1998.

Paterson, W.: The physics of glaciers, Butterworth-Heinemann, 1994.

Pfeffer, W. T., Arendt, A. A., Bliss, A., Bolch, T., Cogley, J. G., Gardner, A. S., Hagen, J.-O., Hock, R., Kaser, G., Kienholz, C., et al.: The Randolph Glacier Inventory: a globally complete inventory of glaciers, Journal of Glaciology, 60, 537–552, 2014.

Radić, V. and Hock, R.: Regional and global volumes of glaciers derived from statistical upscaling of glacier inventory data, Journal of Geophysical Research: Earth Surface, 115, 2010.

Raper, S. C. and Braithwaite, R. J.: Glacier volume response time and its links to climate and topography based on a conceptual model of glacier hypsometry, The Cryosphere, 3, 183–194, 2009.

Rasmussen, L., Andreassen, L., Baumann, S., and Conway, H.: 'Little Ice Age' precipitation in Jotunheimen, southern Norway, The Holocene, 20, 1039–1045, doi:10.1177/0959683610369510, 2010.

Reinardy, B. T., Leighton, I., and Marx, P. J.: Glacier thermal regime linked to processes of annual moraine formation at Midtdalsbreen, southern Norway, Boreas, 42, 896–911, doi:10.1111/bor.12008, 2013.

Rignot, E., Rivera, A., and Casassa, G.: Contribution of the Patagonia Icefields of South America to sea level rise, Science, 302, 434–437, 2003.

Rivera, A. and Casassa, G.: Volume changes on Pio XI glacier, Patagonia: 1975–1995, Global and Planetary Change, 22, 233–244, 1999.

Roe, G. H.: What do glaciers tell us about climate variability and climate change?, Journal of Glaciology, 57, 567–578, 2011.

5 Rutt, I. C., Hagdorn, M., Hulton, N., and Payne, A.: The Glimmer community ice sheet model, Journal of Geophysical Research: Earth Surface (2003–2012), 114, doi:10.1029/2008JF001015, 2009.

Sellevold, M. and Kloster, K.: Seismic measurements on the glacier Hardangerjøkulen, Western Norway, Norsk Polarinslitutt Arbok 1964, pp. 87–91, 1964.

Seppä, H., Hammarlund, D., and Antonsson, K.: Low-frequency and high-frequency changes in temperature and effective humidity during

10 the Holocene in south-central Sweden: implications for atmospheric and oceanic forcings of climate, Climate Dynamics, 25, 285–297, doi:10.1007/s00382-005-0024-5, 2005.

Shepherd, A., Ivins, E. R., Geruo, A., Barletta, V. R., Bentley, M. J., Bettadpur, S., Briggs, K. H., Bromwich, D. H., Forsberg, R., Galin, N., et al.: A reconciled estimate of ice-sheet mass balance, Science, 338, 1183–1189, doi:10.1126/science.1228102, 2012.

Sissons, J.: The Loch Lomond Stadial in the British Isles, Nature, 280, 199–203, doi:10.1038/280199a0, 1979.

15 Sollid, J. and Bjørkenes, A.: Genesis of moraines at Midtdalsbreen, southern Norway, Norsk Geografisk Tidskrift, p. Bd 32, 1978.

Sutherland, D. G.: Modern glacier characteristics as a basis for inferring former climates with particular reference to the Loch Lomond Stadial, Quaternary Science Reviews, 3, 291–309, doi:10.1016/0277-3791(84)90010-6, 1984.

Trüssel, B. L., Truffer, M., Hock, R., Motyka, R. J., Huss, M., and Zhang, J.: Runaway thinning of the low-elevation Yakutat Glacier, Alaska, and its sensitivity to climate change, Journal of Glaciology, 61, 65–75, 2015.

20 Uvo, C. B.: Analysis and regionalization of northern European winter precipitation based on its relationship with the North Atlantic Oscillation, International Journal of Climatology, 23, 1185–1194, doi:10.1002/joc.930, 2003.

Vaksdal, M.: Sammenligning av to dreneringssytemer i Midtdalsbreen, Hardangerjøkulen, Sør-Norge (Comparison of two drainage systems at Midtdalsbreen, Hardangerjøkulen, South Norway). Masters thesis unpublished., Master's thesis, Department of Geography. University of Oslo, Norway, 2001.

25 Van Den Berg, J., van de Wal, R., and Oerlemans, H.: A mass balance model for the Eurasian Ice Sheet for the last 120,000 years, Global and Planetary Change, 61, 194–208, doi:10.1016/j.gloplacha.2007.08.015, 2008.

Vasskog, K., Paasche, Ø., Nesje, A., Boyle, J. F., and Birks, H. J. B.: A new approach for reconstructing glacier variability based on lake sediments recording input from more than one glacier, Quaternary Research, 77, 192–204, doi:10.1016/j.yqres.2011.10.001, 2012.

Vaughan, D., Comiso, J., Allison, I., Carrasco, J., Kaser, G., Kwok, R., Mote, P., Murray, T., Paul, F., Ren, J., Rignot, E., Solomina, O.,

30 Steffen, K., and Zhang, T.: Observations: Cryosphere, In: Climate Change 2013: The Physical Science Basis. Contribution of Working Group I to the Fifth Assessment Report of the Intergovernmental Panel on Climate Change. [Stocker, T.F., D. Qin, G.-K. Plattner, M. Tignor, S.K. Allen, J. Boschung, A. Nauels, Y. Xia, V. Bex and P.M. Midgley (eds.)]. Cambridge University Press, Cambridge, United Kingdom and New York, NY, USA, 2013.

Velle, G., Brooks, S. J., Birks, H., and Willassen, E.: Chironomids as a tool for inferring Holocene climate: an assessment based on six sites

35 in southern Scandinavia, Quaternary Science Reviews, 24, 1429–1462, doi:10.1016/j.quascirev.2004.10.010, 2005a.

Velle, G., Larsen, J., Eide, W., Peglar, S. M., and Birks, H. J. B.: Holocene environmental history and climate of Råtåsjøen, a low-alpine lake in south-central Norway, Journal of Paleolimnology, 33, 129–153, doi:10.1007/s10933-004-2689-x, 2005b.

Weertman, J.: The theory of glacier sliding, Journal of Glaciology, 5, 287–303, doi:10.1007/978-1-349-15480-7_14, 1964.

Willis, I. C.: Intra-annual variations in glacier motion: a review, Progress in Physical Geography, 19, 61–106, doi:10.1177/030913339501900104, 1995.

Willis, I. C., Fitzsimmons, C. D., Melvold, K., Andreassen, L. M., and Giesen, R. H.: Structure, morphology and water flux of a subglacial drainage system, Midtdalsbreen, Norway, Hydrological Processes, 26, 3810–3829, doi:10.1002/hyp.8431, 2012.

5 Winkelmann, R., Martin, M., Haseloff, M., Albrecht, T., Bueler, E., Khroulev, C., and Levermann, A.: The Potsdam parallel ice sheet model (PISM-PIK)–Part 1: Model description, The Cryosphere, 5, 715–726, doi:10.5194/tc-5-715-2011, 2011.

Woo, M.-k. and Fitzharris, B.: Reconstruction of mass balance variations for Franz Josef Glacier, New Zealand, 1913 to 1989, Arctic and Alpine Research, pp. 281–290, 1992.

Zekollari, H. and Huybrechts, P.: On the climate–geometry imbalance, response time and volume–area scaling of an alpine glacier: insights
10   from a 3-D flow model applied to Vadret da Morteratsch, Switzerland, Annals of Glaciology, 56, 51, doi:10.3189/2015AoG70A921, 2015.

Zekollari, H., Huybrechts, P., Furst, J. J., Rybak, O., and Eisen, O.: Calibration of a higher-order 3-D ice-flow model of the Morteratsch glacier complex, Engadin, Switzerland, Annals of Glaciology, 54, 343–351, doi:10.3189/2013AoG63A434, 2013.

Zekollari, H., Furst, J. J., and Huybrechts, P.: Modelling the evolution of Vadret da Morteratsch, Switzerland, since the Little Ice Age and into the future, Journal of Glaciology, 60, doi:10.3189/2014JoG14J053, 2014.

15 Ziemen, F. A., Hock, R., Aschwanden, A., Khroulev, C., Kienholz, C., Melkonian, A., and Zhang, J.: Modeling the evolution of the Juneau Icefield between 1971 and 2100 using the Parallel Ice Sheet Model (PISM), Journal of Glaciology, 62, 199–214, 2016.
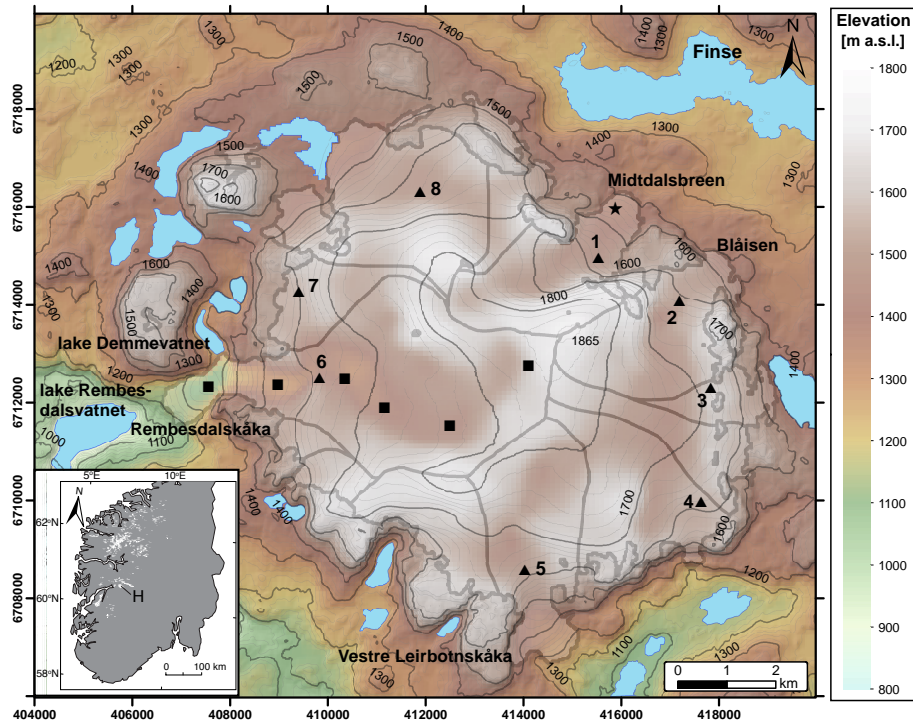
Figure 1. Bed (coloring) and surface (contours) topography of Hardangerjøkulen ice cap. Contour interval is 20 m and created from a digital elevation model by Statens Kartverk, 1995. The reference system is UTM zone 32N (EUREF89). Ice cap outline and drainage basins from 2003 are indicated (data from Cryoclim.net), as well as surrounding lakes (drawn after Statens Kartverk N50 1:50 000). Shown are GPS positions for velocity measurements (numbered triangles), mass balance stakes from NVE (squares) and location of the automatic weather station (star). Inset: map of southern Norway showing the location of Hardangerjøkulen (H).

Table 1. Constants and parameter values used in this study.

Parameter	Symbol	Unit	Value
Ice density	ρ_i	kg m^{-3}	917
Gravitational acceleration	g	m s^{-2}	9.81
Flow factor	A	s^{-1} Pa^{-3}	0.95×10^{-24} to 2.4×10^{-24}
Sliding parameter	β	m s^{-1} Pa^{-1}	4×10^{-12} to 1×10^{-13}
Sliding law exponent	m		1
Glen's law exponent	n		3
Mesh resolution	Δx	m	200-500
Time step	Δt	a	0.02
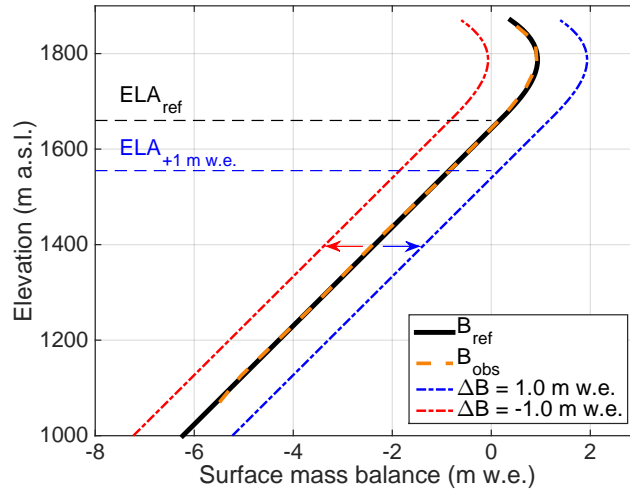
Figure 2. Reference net surface mass balance (B_{ref}) profile used in the model runs, based on the mean observed (B_{obs}) profile for 35 of the 45 years 1963-2007. At lower elevations, a linear gradient is used; for the highest elevations, a third-order polynomial is fitted to the observed values. Shown are also $\Delta B(t)$ = -1.0 and +1.0 m w.e., examples of how temporal mass balance changes are imposed (Eq. 6), along with corresponding ELA's. For -1.0 m w.e., mass balance is negative at all elevations, thus ELA is above the summit. Data from NVE.
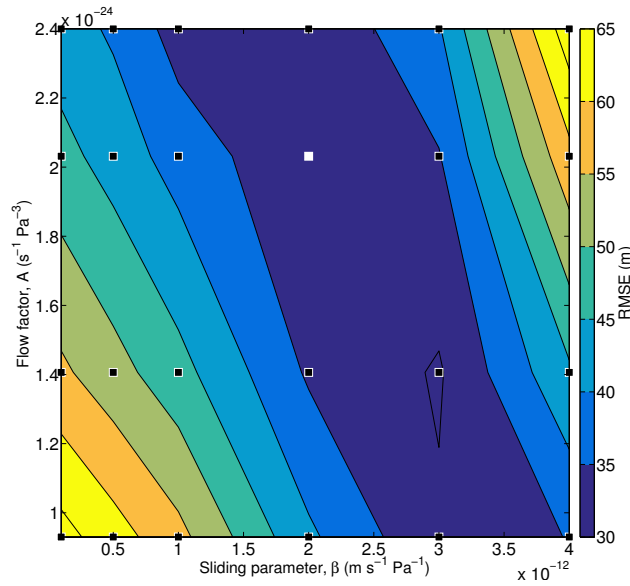
Figure 3. Root mean square error (RMSE) between modelled and observed present-day ice thickness along the flowlines of Midtdalsbreen and Rembesdalskåka, using an ensemble of sliding (β) and rheology (A) parameters. Shown are parameter combinations (black squares) and the 'best-fit' parameter combination used in subsequent runs (white square).
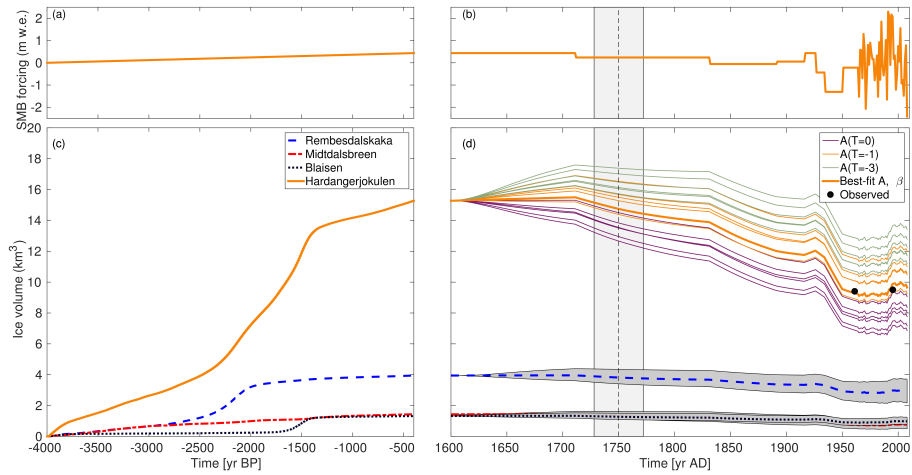
Figure 4. (a) Mass balance forcing for mid- to late Holocene (spinup period), and for (b) 1600 - 2008 AD. (c) Ice volume response for mid- to late Holocene and for (d) 1600 - 2008 AD using an ensemble of sliding and deformation parameter combinations (dark shading) and our 'best-fit' combination obtained from independent calibration. Colors represent different outlet glaciers and the whole ice cap. The LIA maximum, as dated at Midtdalsbreen(dashed line), and its temporal uncertainties (light shading) is also shown, as well as ice volume observations from 1961 and 1995 (black dots). For details, see text.
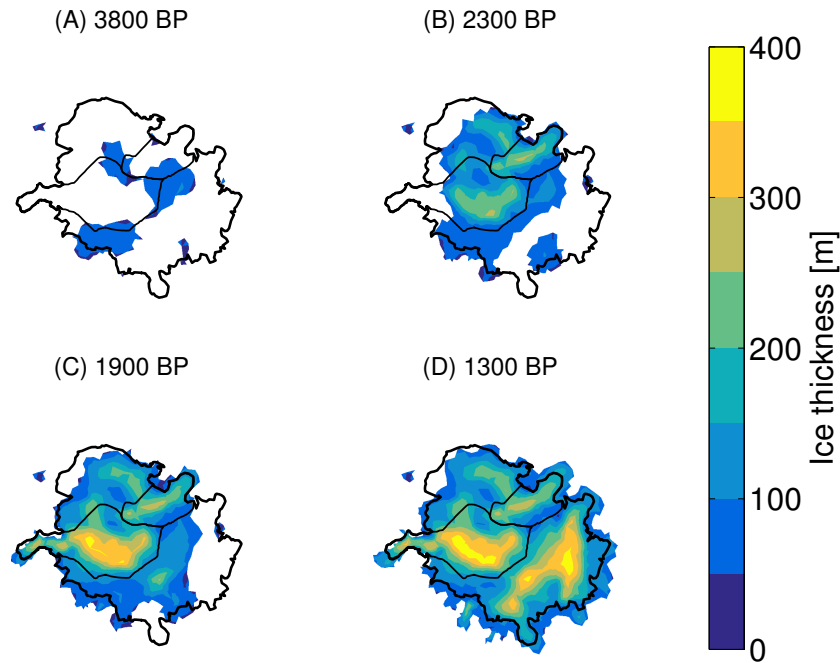
Figure 5. Modelled ice thickness at (A) 3800, (B) 2300, (C) 1900 and 1300 BP using our 'best-fit' model parameters obtained from in-dependent calibration. Shown are also ice cap extent in 1995 AD (black thick line) and corresponding drainage basins for outlet glaciers Rembesdalskåka (SW) and Midtdalsbreen (NE; black thin lines)
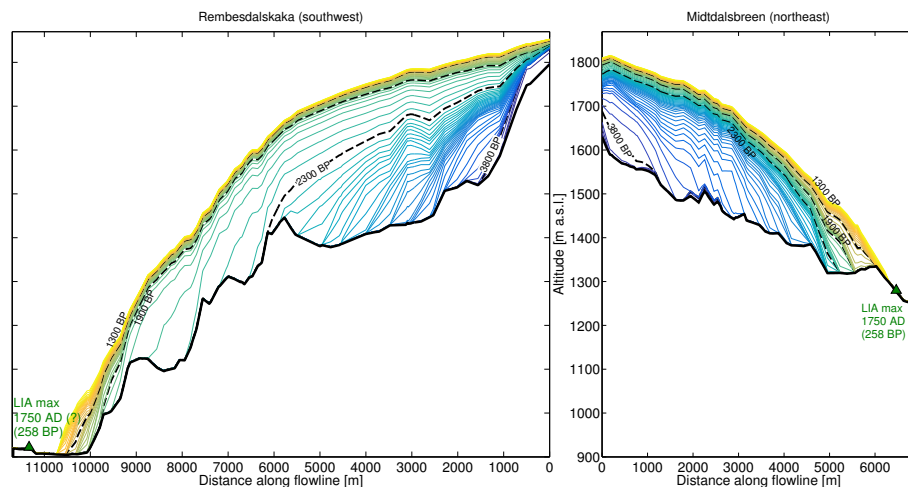
Figure 6. Modelled surfaces from 4000 BP to 1600 AD, starting with no ice cap, shown every 50 years from older (dark blue) to younger (yellow). BP ages are relative to 2008 AD. Note that the top of Rembesdalskåka (Hardangerjøkulen's summit) does not coincide with the top of Midtdalsbreen's flowline (see Fig. 9d).
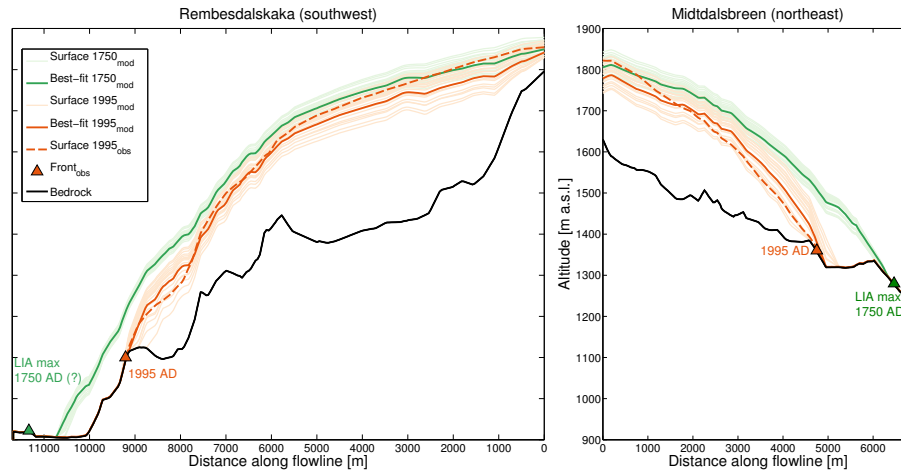
Figure 7. Modelled surfaces for 1750 (light green) and 1995 AD (light orange) for Rembesdalskåka and Midtdalsbreen, using an ensemble of different dynamical parameter combinations. Modelled surface using our 'best-fit' parameter combination is also shown for 1750 (green) and 1995 (orange), as well as observed surface in 1995 (dashed orange). Outlet front positions as known from dated (Midtdalsbreen) and assumed contemporary (i.e. not dated; Rembesdalskåka) terminal moraines are indicated with triangles. Note that the top of Rembesdalskåka (Hardangerjøkulen's summit) does not coincide with the top of Midtdalsbreen's flowline (Fig. 9e).
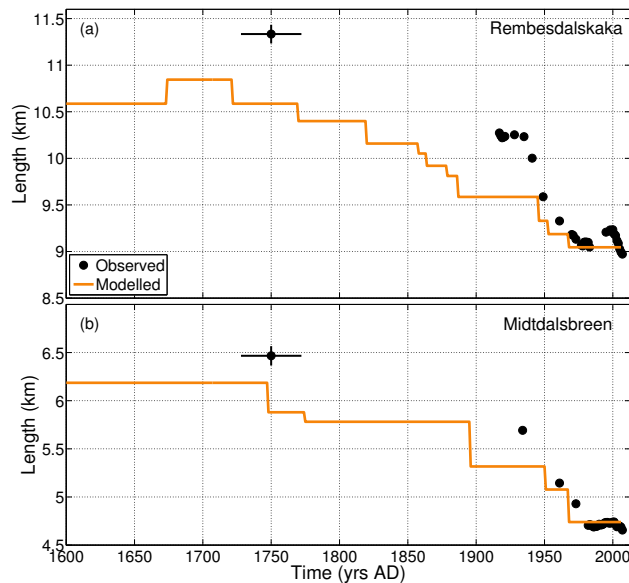
Figure 8. Modelled and observed length of outlet glaciers (a) Rembesdalskåka and (b) Midtdalsbreen. Temporal uncertainty for 1750 is indicated based on a 10 % age error (Innes, 1986) on the dated moraine at Midtdalsbreen (Andersen and Sollid, 1971), and assuming that the Rembesdalskåka moraine is contemporary. Uncertainties in measured lengths in the 1900s and 2000s are smaller than the marker size.
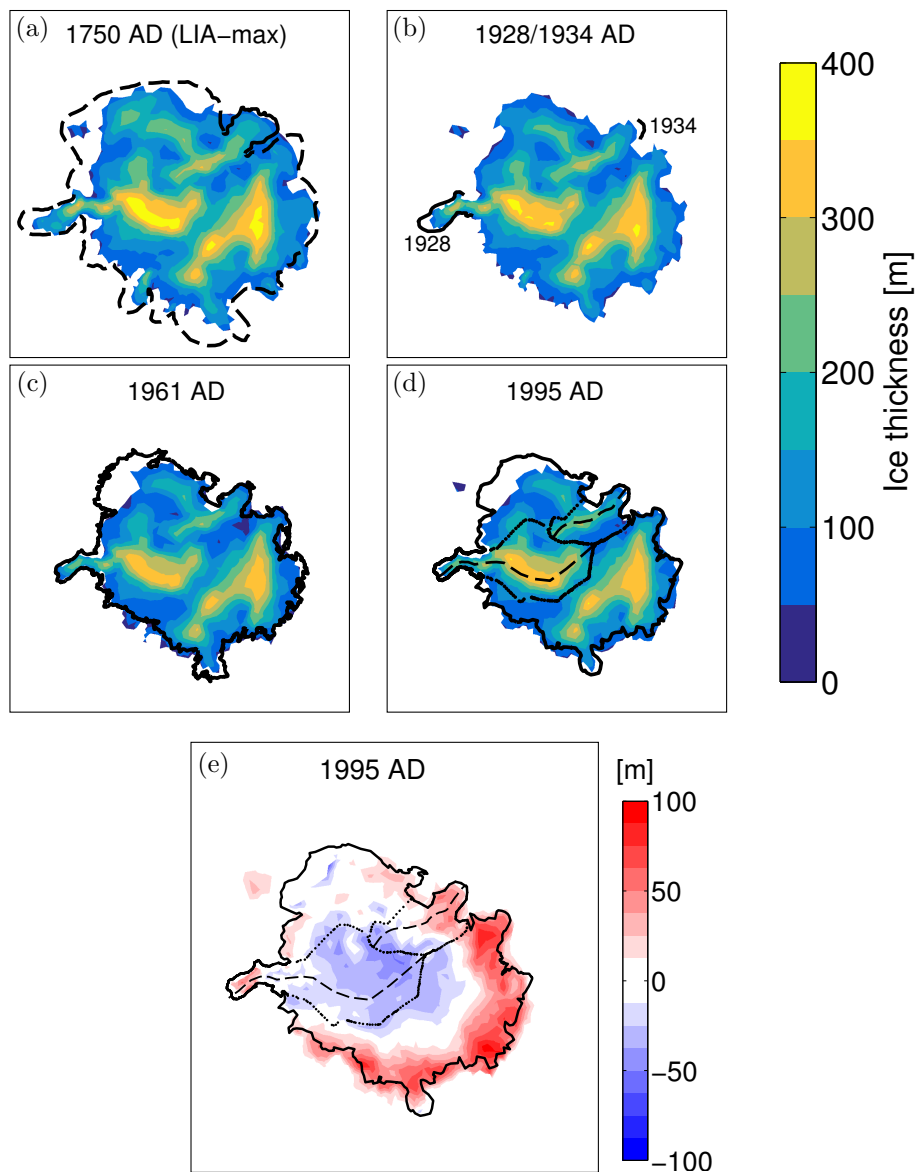
Figure 9. Modelled ice thickness of Hardangerjøkulen in (a) 1750, (b) 1928, (c) 1961 and (d) 1995 AD. Shown is also the difference between modelled and observed surface in 1995 (e), where positive (negative) values indicate that the model overestimates (underestimates) surface elevation. Observed ice cap extents (Andersen and Sollid (1971); Sollid and Bjørkenes (1978); A.Nesje, pers. comm; H. Elvehøy, pers. comm; Cryoclim.net/NVE) for corresponding years are shown where available. For 1750, assumed LIA extent from geomorphological evidence (dashed line) and dated LIA extent (solid line) is shown. For 1928/1934, the modelled thickness displayed is for 1928, though the observed front shown for Mitdalsbreen is from 1934. Drainage basins and flowlines of Rembesdalskåka and Midtdalsbreen are shown for 1995.
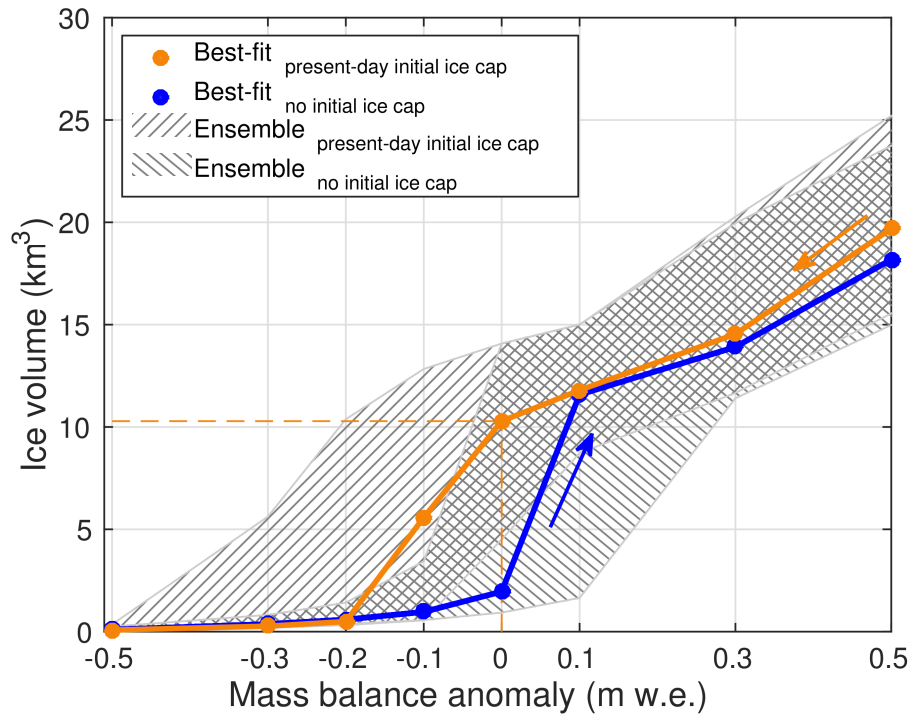
Figure 10. Steady-state ice volumes reached using step perturbations of the 1963-2007 mass balance, using an ensemble of dynamical parameter combinations, starting from the present-day ice cap and ice-free conditions.
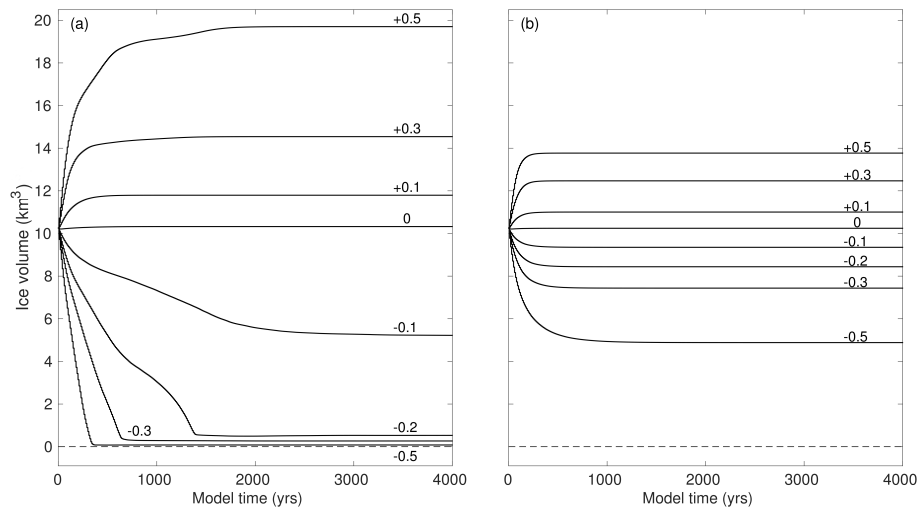
Figure 11. Ice volume evolution for selected mass balance perturbations (-0.5 to 0.5 m w.e.) relative to the mean mass balance 1963-2007, using our 'best-fit' dynamical parameter combination, for (a) with and (b) without a mass balance-altitude feedback. A mass balance anomaly of -0.2 m w.e. is added for greater detail of when Hardangerjøkulen disappears.
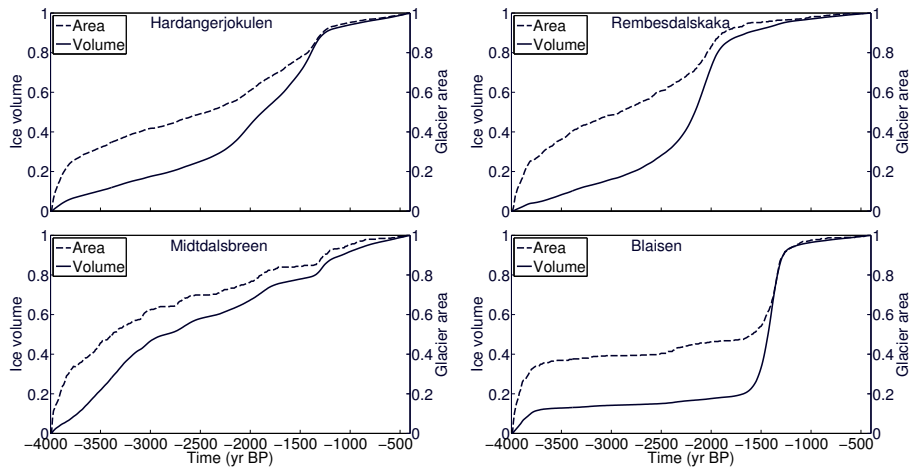
Figure 12. Simulated ice volume and area evolution for (a) Hardangerjøkulen, and the outlet glaciers (b) Rembesdalskåka, (c) Midtdalsbreen, and (d) Blåisen, from 4000 to 400 BP (1600 AD). Quantities are non-dimensionalized relative to final volume and area in year 1600 AD, respectively.
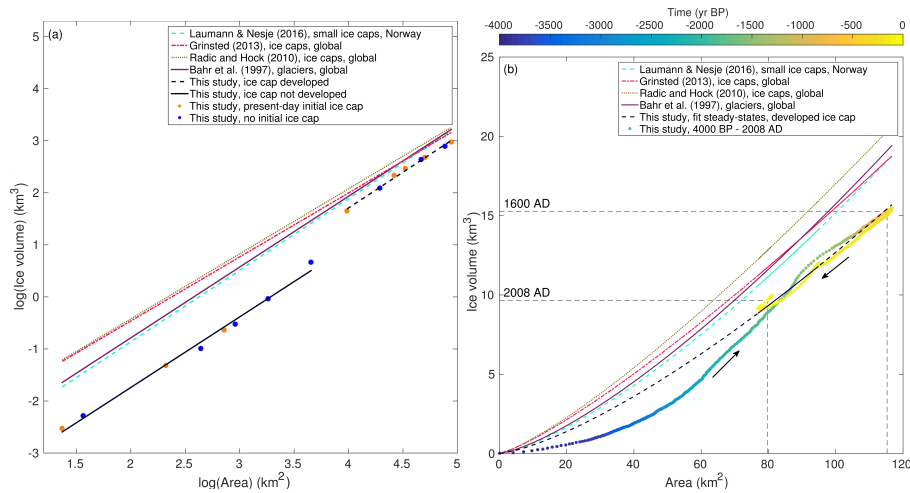
Figure 13. (a) Logarithmic values of volume and area for steady-state experiments using mass balance anomalies within -0.5 to +0.5 m w.e. relative to the 1963–2007 AD reference mass balance. Both steady-states reached from the present-day ice cap and from ice-free conditions are shown. Steady-states are grouped into two cases, depending on whether an ice cap has developed or if ice is only present on high ridges. Commonly used volume-area relations from the literature are also shown (Bahr et al., 1997; Radić and Hock, 2010; Grinsted, 2013; Laumann and Nesje, 2016). (b) Volume and area combinations for our simulation from 4000 BP to 2008 AD, along with the volume-area relation derived from simulated developed steady-state ice caps in (a).
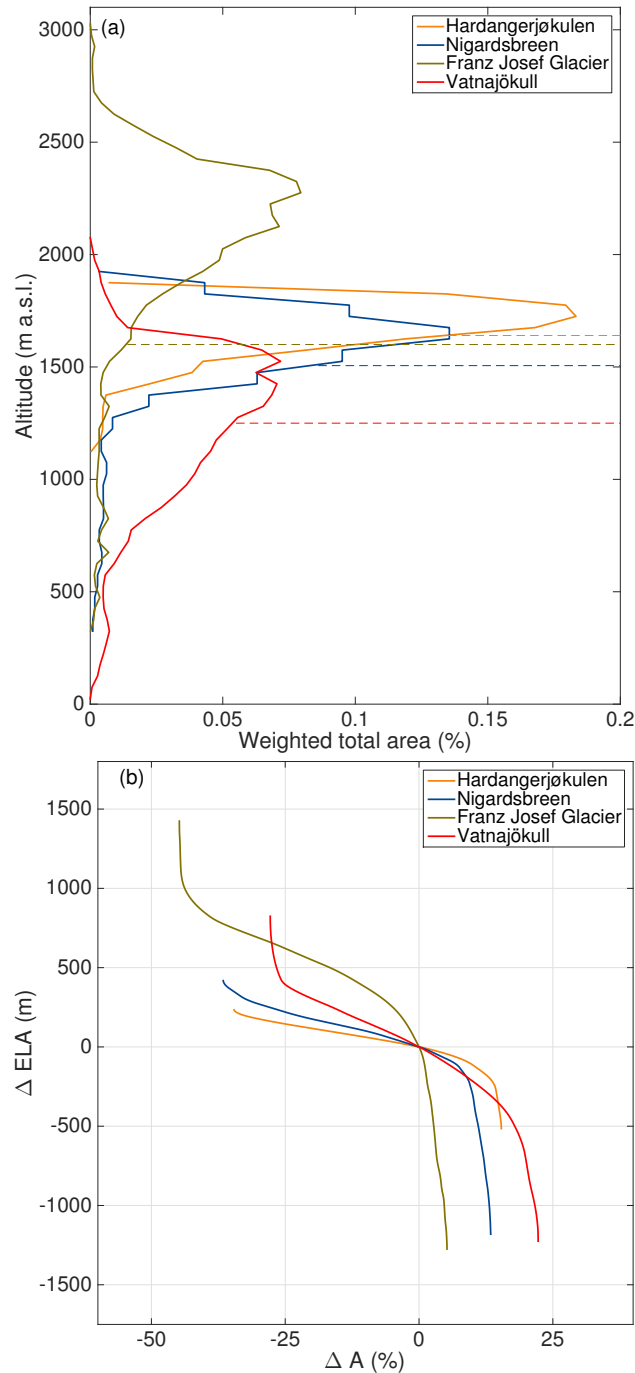
Figure 14. (a) Hypsometry of present-day Hardangerjøkulen (Giesen and Oerlemans, 2010) and Nigardsbreen, Norway (Oerlemans, 1997a), Franz Josef Glacier, New Zealand (Woo and Fitzharris, 1992) and Vatnajökull, Iceland (Aðalgeirsdóttir et al., 2003). Respective ELAs are indicated with dashed lines. Areas are weighted by the total area, and altitude bins are 25 m. (b) Effect of a step change in ELA on area for respective glacier.